May 2021

Visually Guided Action for the Person-Plus-Object System: Generalizing the Optic Flow Equalization Control Law to Asymmetrical Bodies

Kathryn Lucaites
Clemson University, klucaites@comcast.net

VISUALLY GUIDED ACTION FOR THE PERSON-PLUS-OBJECT SYSTEM: GENERALIZING THE OPTIC FLOW EQUALIZATION CONTROL LAW TO ASYMMETRICAL BODIES

A Dissertation
Presented to
the Graduate School of
Clemson University

In Partial Fulfillment
of the Requirements for the Degree
Doctor of Philosophy
Human Factors Psychology

---

by
Katie Lucaites
May 2021

Accepted by:
Dr. Christopher Pagano, Committee Chair
Dr. Rick Tyrrell
Dr. Patrick Rosopa
Dr. Andrew Robb

Abstract

Visually guided action in humans occurs in part through the use of control laws, which are dynamical equations in which optical information modulates an actor's interaction with their environment. For example, humans locomote through the center of a corridor or through the center of two obstacles by equalizing the speed of optic flow across their left and right fields of view. This optic flow equalization control law relies on a crucial assumption: that the shape of the body relative to the eyes is laterally symmetrical. Humans engaging in tool use are often producing person-plus-object systems that are not laterally symmetrical, such as when they hold a tool, bag, or briefcase in one hand, or when they drive a vehicle. This dissertation tests a new generalized control law for centered steering that accounts for asymmetries produced by external tool use. Experiment 1 tested the efficacy of the generalized control law in a replication of Duchon & Warren (2002). Participants held an asymmetrical bar and centered themselves within a virtual moving hallway while the speed of the virtual walls were systematically changed. Experiment 2 assessed the application of the generalized control law to an aperture passability task, in which participants holding asymmetrical bars walked through real world apertures of various widths. The results of the current studies demonstrate that humans engaging with an asymmetrical tool can 1) perceive the asymmetry of a person-plus-object system, 2) use that information to modulate the use of optic flow equalization control laws for centered steering, and 3) functionally incorporate the asymmetrical tool into their perception-action system to successfully navigate their environment with a 97% success rate.

Acknowledgements

This project would not have been possible without the support of numerous individuals. I would like to extend my sincerest appreciation and respect to all who shared their time, effort, and ideas to make this dissertation a success.

I am extremely grateful to Roshan Venkatakrishnan and Rohith Venkatakrishnan, who were instrumental in developing the virtual reality environment and motion tracking software. Thank you for producing high quality work under immense time pressure – when Covid-19 threatened to put an uncertain deadline on data collection, your long hours and late nights saved the day. I also gratefully acknowledge Chloe Craft, Aubrey Hodapp, and Kelsey Quinn for their support with pilot testing and data collection. Learning any research protocol becomes more complicated with the addition of Covid-19 safety procedures - thank you for your bravery, professionalism, and willingness to help.

I would also like to thank my past and present lab mates for their enduring support and encouragement. To Brian Day and Leah Hartman, thank you for being the most incredible role models, and for having confidence in my abilities from the very start. You both have impacted my growth in more ways than you know. To Hannah Solini, thank you for being a welcoming soundboard for my ideas. It has been a pleasure working alongside such a bright scientist, and I truly value our friendship.

I would like to extend my sincerest gratitude to my committee members, Dr. Rick Tyrrell, Dr. Patrick Rosopa, and Dr. Andrew Robb. Each of you supported the development and execution of this project in different ways. Thank you for challenging me, encouraging me, and sharing your ideas. This dissertation is better because of each of

you. Lastly, my graduate success would not have been possible without the support of my advisor, Dr. Chris Pagano. Chris - thank you for developing a lab that feels less like work and more like family, thank you for introducing me to the world of ecological psychology, and thank you for perfectly balancing the guidance and freedom I needed to grow into the researcher I am today. My time with you at Clemson has been the most incredible learning experience.

Table of Contents

List of Tables

List of Figures

List of Equations

CHAPTER I

Introduction

> "Locomotion and manipulation are neither triggered nor commanded but *controlled*… They are controlled not by the brain, but by information… Control lies in the animal-environment system… Behavior is regular without being regulated. The question is how this can be." (J.J. Gibson, 1979, p. 225)

In more ways than we often appreciate, the ability to move about and interact with the environment is crucial to the safe and efficient completion of daily activities. Controlled locomotion is so crucial to one's safety and well-being that it provides a noticeable adaptive advantage. Without the ability to move in a controlled and directed manner, an animal cannot consistently or effectively hunt, forage, prey, migrate, avoid predators, mate, or conduct other activities that "implement the circumstances for furthering one's kind" (Turvey, 2019).

The prevalence of successful perception-action systems in nearly every life form - from single-celled organisms, to insects, to humans – suggests that a cognitively taxing representational approach is unlikely to underly perception-action processes. Alternatively, the ecological approach to perception and action uses empirical research to identify optical variables that directly specify meaningful information about one's environment. According to this approach, structured light can both inform an actor about their relationship to the environment and guide the actor's movement through the environment. The present work is directed at further understanding how actors use optical information to guide their locomotion.

Visually Guided Action and the Importance of Optic Flow

In order to understand how organisms engage with their environments, it is first crucial to understand how visual perception is linked to the control of action (J. J. Gibson, 1958; Warren, 1998). Visual information about the environment allows for prospective control, which is the ability to guide future-oriented actions such as avoiding obstacles (J. J. Gibson, 1979; Reed, 1996; Turvey, 1992).

The ecological approach to perception and action starts with an analysis of the surfaces, objects, and animals that make up an environment, along with an optical analysis of how information about the environment can be conveyed lawfully to the observer through energy arrays (J. J. Gibson, 1950, 1966, 1979; Turvey et al., 1981). For visual perception, the energy array of interest is generated by the reflection and refraction of radiant light. A light source (radiant light) illuminates an environment and is structured by the scatter-reflection of light upon all surfaces of that environment. The result of this is a perceivable ambient optic array surrounding an optical structure (i.e., eye). James Gibson's seminal research on 'ecological optics' worked to identify meaningful information in the ambient optic array, that is, ways in which the surfaces and substances of the environment lawfully structure the light comprising the optic array (J. J. Gibson, 1950, 1961, 1979). This approach suggests that perceivers can pick up information about the environment without the need for elaboration by a cognitive entity.

J.J. Gibson (1950) also acknowledged that in everyday life, the ordinary stimulus for vision was not a still image-like optic array, but instead a 'deformation' of the visual field caused by motion of the observer. Indeed, motion of the observer or motion of

objects in the environment produces a lawful transformation of the optic array. This pattern of motion on the retina is called optic flow, and can be described in terms of velocity vectors of light on the retina (J. J. Gibson, 1950; Koenderink, 1986; Lee, 1980).

Patterns of optic flow provide information about the types of motion that produced them. For example, self-motion of the observer is indicated by a global transformation of the optic array. During forward translational movement, the entire optic array expands outward from a singular focus point, and the direction of movement is specified by the location of the optic flow field from which motion vectors radiate (focus of expansion). During rotational movement, the entire optic array sweeps across the eyes in the opposite direction of rotation. These and other patterns of optic flow specify the types and qualities of motion in the environment so much so that Gibson makes the following proclamation:

> "So strict are the geometric relationships between physical motion of the observer's body and retinal motion of the projected environment that the latter provides in fact the chief sensory guide for locomotion in space. Retinal deformation is actually a kind of visual kinesthesis." (J.J. Gibson, 1950, p. 124)

By visual kinesthesis, Gibson refers to the perception of the observer's movement that can be detected purely through optical information. While bodily motion can be perceived using other sensory systems, such as the vestibular and somatosensory systems, the visual system is the most robust system to accurately convey movement information across all active and passive forms of self-motion (J. J. Gibson, 1966). Indeed, optic flow fields provide such rich information about self-motion that artificial perturbations to optic flow patterns have been shown to impact postural control (Lee & Aronson, 1974;

Lishman & Lee, 1973), walking speed (Prokop et al., 1997; Schubert et al., 2005), distance perception (Durgin et al., 2005; Rieser et al., 1995; Solini et al., 2021), steering behavior (Sarre et al., 2008), and accuracy for pointing to a target (Hartman, 2018).

Control Laws: How Optic Flow Guides Emergent Behavior

Because patterns of optic flow directly specify characteristics of the motion that produced them, they can be used to control behaviors of the observer. That is, specific patterns of self-movement can be controlled by manipulating the body in such a way as to generate a specific pattern of optic flow (J. J. Gibson, 1958). To approach an object, move in such a way that the object is the focus of expansion (e.g., the optic array radiates outwards from the object); to stand still, move in such a way that the global optic flow is cancelled; to turn, move in such a way that the focus of expansion is shifted to a new patch in the optic array; and so on. These formulas were first described by Gibson as "rules for the visual control of locomotion" (J. J. Gibson, 1979), and are now best known as "control laws" (Warren, 1988; Warren & Fajen, 2004).

Control laws characterize the ways in which information from optic flow can be used to guide actions such as steering towards goals, avoiding obstacles, and chasing moving objects. With control laws, behavior is controlled "on-line" by coupling motor activity to current visual information rather than generating motor commands from internally constructed models of the world and the actor's current state (Zhao & Warren, 2015). Instead of generating formulas that specify kinematic or kinetic variables as a function of optic flow, control laws are written such that the optic flow modulates the dynamic actor-environment system (Warren & Fajen, 2004).

Dynamical systems consist of a large number of interacting components that exhibit emergent, self-organized behavior (Guastello et al., 2009; Riley & Van Orden, 2005). That is, behavior is not determined by a central controller, but rather emerges from the interactions between system components. Consider the actor-environment system. The actor's body consists of the central nervous system, neurons, joints, muscles, motor units, an endocrine system, a digestive system, and so on. Further, the actor is embedded within a complex environment, consisting of structures, objects, animals, air, forces, and so on. It is the interactions between all of these components that ultimately determines the behavior of the system.

Dynamical systems can be described by assessing their location in phase space, which are the coordinates formed by all dynamic variables of the system. Attractors are subsets of the state space towards which the trajectory of the dynamical system is drawn, while repellors are subsets of the phase space from which the trajectory is pushed away. For the actor-environment system, behavioral constraints such as the structure of the environment, biomechanics of the body, available perceptual information, and task demands serve as attractors and repellors for the system (Warren, 2006). Considering this, control laws specify attractors and repellors for the action system that promote emergent and adaptive behaviors (Fajen, 2007; Warren & Fajen, 2004).

J. J. Gibson & Crooks (1938) exemplified the idea of attractors and repellors in their description of the "field of safe travel" for automobile drivers. They argued that obstacles in the roadway (e.g., pedestrians, other vehicles, etc.) had 'negative valences' by which the path of the automobile moved away from (e.g., was repelled away from),

while task goals like the destination of travel had 'positive valences' by which the path of the vehicle moved towards (e.g., was attracted to). Dynamic control laws relating goal-oriented locomotion to patterns of optic flow work in similar ways. Control laws have been applied to explain postural control (Warren et al., 1996), steering (Lee & Lishman, 1977), and braking (Lee, 1976; Yilmaz & Warren, 1995) in human walking, as well as flight control in insects (Collett & Land, 1975; Wagner, 1982, 1986), and have been used more recently to guide behavior-based control in autonomous robots (Duchon et al., 1998; Duchon & Warren, 2002, 1994).

Optic Flow Equalization

Consider the control law used to travel in a straight-line path through the center of a corridor, or through the center of two obstacles. The desired pattern of optic flow is an equal speed of optic flow to the left and right of the focus of expansion, as seen in Equation 1.

Equation 1

Original Optic Flow Equalization Control Law from Duchon et al., 1998

$$\Delta(F_L - F_R) = k\,(v_r - v_l)\,,\ \text{where}$$

F is the amount of force applied in each direction, resulting in lateral translations,

k is an optical scaling coefficient,

v is the horizontal angular velocity of optical flow.

This control law relies on the principle of motion parallax, which states that the angular velocity at which objects in the environment move across the optic flow field during observer self-motion is lawfully related to the object's relative distance from the observer (E. J. Gibson et al., 1959; Helmholtz, 1925). Objects in the optic flow field moving faster across the retina are a closer distance from the observer than objects moving slower across the retina. Therefore, if an actor equalizes the speed of optic flow across the left and right eyes, they also equalize their distance to the surfaces of the environment in the left and right visual field.

Early research about the efficacy of the optic flow equalization control law studied the flight paths of honeybees through corridors with black and white gratings on the walls (Srinivasan, 1992, 1998; Srinivasan et al., 1991). When both walls had matching grating patterns, bees flew down the center of the corridor, equally distant from both walls. When one of the walls was moved in the same direction as the bee's flight, the angular velocity of optic flow from that wall was reduced when the bee flew down the center, causing the bees to steer their path toward the moving wall in order to satisfy the control law of flow equalization. Opposite results were found when one wall moved in the opposite direction as the bee's travel: the speed of optic flow from the moving wall was increased, and the bees steered away from the moving wall in order to reduce the angular velocity of the moving wall and maintain the control law.

Interestingly, changing one wall's grating pattern to a higher spatial frequency did *not* impact the flight patterns: bees traveled down the center when the walls were still and shifted their lateral position when one wall was moving. This suggests that the bees were

indeed balancing the speed of the optic flow instead of relying upon other visual cues, such as the contrast frequency (Srinivasan et al., 1991).

Similar experiments conducted with birds (Bhagavatula et al., 2011) and humans (Chou et al., 2009; Duchon & Warren, 2002; Kountouriotis et al., 2013; Sarre et al., 2008) have shown the same optic flow equalization strategy in use. Duchon & Warren (2002) placed participants in front of a large screen depicting a virtual hallway and asked them to move down the center of the hallway by either using a joystick or walking on a treadmill. When the speeds of the left and right walls differed, both modes of locomotion produced behaviors that were consistent with the optic flow equalization strategy, with participants traveling 66-85% of the predicted distance. The use of this control law is found even when explicit path boundaries are visible (Duchon & Warren, 1994; Kountouriotis et al., 2013).

Affordances: Perceiving a Meaningful Environment

It is important to note that in order to utilize optical control laws, one must have the agency to determine a goal and self-initiate an action (Warren, 1988). Optic flow equalization is only a useful mechanism for action if the actor intends to walk through a corridor. If the actor instead intends to intercept or avoid a moving object, a different optical control law would be used. In any given scenario, the actor-environment system offers many possibilities for action. These action capabilities, or affordances, are determined by the relationship between properties of the environment and properties of the action system (J. J. Gibson, 1979). Importantly, affordances are perceived directly. That is, objects and surfaces of the environment are optically specified as intrinsic units

of the actor's morphology (body-scaling) and dynamic capabilities (action-scaling). Affordances reveal the underlying meaning of the environment, and are crucial for an actor's successful interaction with the environment.

The remainder of this paper will focus on aperture passability, which is the affordance for locomoting through apertures or openings. Individuals determine their ability to pass through an aperture by comparing the width of the opening with their widest frontal dimension - their shoulder width. Warren and Whang (1987) found that regardless of body size, humans use intrinsic scaling of their own geometric dimensions to determine if an aperture affords passing. When asked to walk through a series of doors at a natural pace, participants made no changes to their gate if the aperture was sufficiently larger than the participant's shoulder width. But when the size of the aperture was 1.3X the participant's shoulder width or smaller, participants chose to turn their shoulders when passing through the aperture. By turning their shoulders, participants reduced their frontal width and created a safety buffer, which reduced the likelihood of collision caused by movement variability generated while walking (Franchak et al., 2012; Hackney & Cinelli, 2013; Higuchi et al., 2011; Lucaites, Venkatakrishnan, Bhargava, et al., 2020; Wagman & Malek, 2007; Wilmut et al., 2015).

Importantly, one's affordance perception is sensitive to artificial changes in body size and shape due to external tool use (Day et al., 2017). When holding a tool that extends the frontal dimensions of the body, actors rely on the person-plus-object (PPO) system to determine their aperture passability (Wagman & Taylor, 2005). That is, the actor must scale their environment in relation to the affordances offered by the new

morphology and dynamic capabilities generated by the actor's interaction with the tool. For aperture passability, this means that determining passability requires a comparison of the aperture width to the widest frontal dimension, whether that is comprised of the boundaries of the shoulders, the boundaries of the tool, or a combination of both. Actors have successfully perceived their affordances for aperture passability across a variety of body-extending tools including hand-held objects (Hackney et al., 2014; Wagman & Malek, 2007; Wagman & Taylor, 2005), shoulder pads (Higuchi et al., 2011), wheelchairs (Higuchi et al., 2004, 2006, 2009; Lucaites, Venkatakrishnan, Venkatakrishnan, et al., 2020), assistive walking devices (Lucaites, 2018), and backpacks (Petrucci et al., 2016).

One way to maximize safety when passing through apertures is to ensure that the person-plus-object system is centered between the two sides of the aperture when they pass through. By centering the system within the aperture, the actor can maximize the distance between the most extreme lateral parts of the system and the aperture on both the left and right sides, which minimizes the overall chances of collision. Indeed, deviation from the center of the aperture is a predictor of collision and failed passing (Muroi & Higuchi, 2017), and this variable is often used as a metric of perception/action coordination during the passability task.

Centering the body within an aperture is completed in part by using optic flow equalization: in order to center the body in the aperture, one should equalize the flow speed of the left and right sides of the aperture, see Figure 1. Evidence from eye-tracking experiments suggests that actors fixate their gaze through the center of the aperture (as

opposed to fixated on the edges of the aperture) during the final stages of their approach (Cinelli et al., 2009), and that these fixations are considerably longer in duration than those earlier in the approach phase (Higuchi et al., 2009). This suggests that participants were relying on optic flow to guide them through the center of the door.

Figure 1

Optic Flow Equalization as a Strategy for Aperture Passability

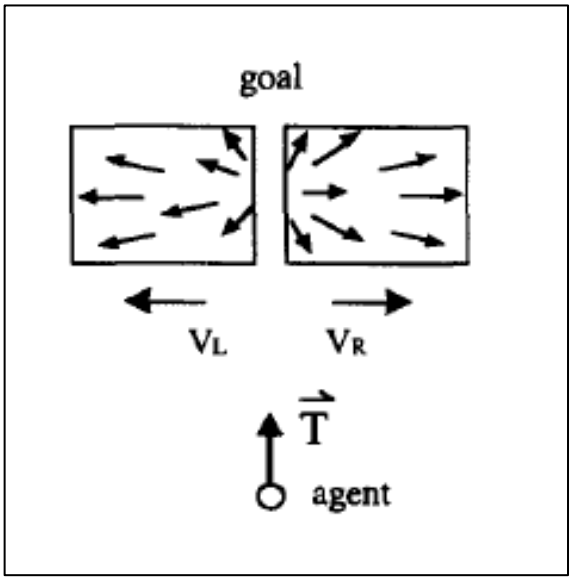

Note. Image from Warren (1988).

Bilateral Symmetry as an Assumption of Optic Flow Equalization

The optic flow equalization strategies used to guide passage through an aperture or corridor rely on a very crucial assumption: that the shape of the body relative to the eyes is laterally symmetrical. Equalizing optic flow on either side of the point of observation ensures that an actor will navigate through the center of an aperture or

corridor *only* if their body extends an equal distance outward from their left and right eyes. If one's body morphology was asymmetrical, protruding further to the right than to the left of the midpoint of the eyes, then adjustments would need to be made to the flow equalization control law used to guide locomotion. Similarly, in order for an actor to utilize flow equalization to pass through the center of an aperture within the person-plus-object system, the object itself must be positioned in such a way that it is laterally symmetrical with reference to the actor's eyes.

Animal morphologies displaying bilateral symmetry originated in the Precambrian Eon (Knoll & Carrol, 1999), and today over 99% of all animal species exhibit bilateral symmetry. Hypotheses attempting to explain the adaptive advantage of symmetry suggest that it originated as a locomotor advantage for aquatic creatures. Bilateral symmetry ensured that environmental pressures (e.g., drag, resistance, etc.) on both sides of the body were equalized, which allowed for linear motion if the body was held in a straight position and quick changes in direction if the body was bent to eliminate the symmetry (Holló & Novák, 2012). Proponents of the ecological approach would point out that an additional adaptive advantage of bilateral symmetry is that it allowed animals to develop simple control laws that rely on the equalization of *information* picked up by perceptual organs.

Humans engaging in tool use are often producing person-plus-object systems that are not laterally symmetrical, such as when they hold a tool, bag, or briefcase in one hand, or when they drive a vehicle or a motorbike with a sidecar. In these cases, the

midpoint of the body and the midpoint of the PPO are not the same, and thus optic flow equalization cannot be used to center the PPO through an aperture.

Little research has been conducted to assess the effects of an asymmetrical PPO on an actor's ability to walk down corridors or pass through apertures. Wagman & Taylor (2005) assessed perceptions of passability while participants held T-shaped bars of differing lengths, but each bar was symmetrical to the participant. Kroll & Crundall (2019) conducted an eye-tracking study of firetrucks navigating narrow roadways. Indeed, driving a vehicle is a common example of an asymmetrical person-plus-object system. However, the video stimuli used for the experiment were filmed from the midpoint of the firetruck instead of from the driver's seat perspective, thereby eliminating the asymmetry of the truck. Lastly, Higuchi et al. (2015) compared passability performance for PPOs that were centered and "off the center" to the right and found that participants were able to successfully complete both tasks, although the off-center condition produced more initial collisions with the aperture. However, this research only studied one instance of asymmetry, and only in one direction. To better understand how controls laws can be used to guide aperture passability, a generalization of the optic flow equalization strategy to PPO asymmetry is required.

Generalizing Optic Flow Equalization to Account for Bilateral Asymmetry

Recall the optic flow equalization formula for symmetrical bodies, in which the body is centered when the speed of optic flow to the left and right field of view is equal (see Equation 1). A minor adjustment to this control law allows for successful steering of an asymmetrical body. When the body is not symmetrical relative to the eyes, the optical

flow pattern required for steering down the center of a corridor or aperture must take into account the proportion of the body on the left and right sides of the eyes, as well as the total frontal width of the body (or person-plus-object system). Consider the example in Figure 2, in which ¼ of the body extends to the left of the eyes and ¾ of the body extends to the right of the eyes. If the actor utilized optic flow equalization alone (Figure 2-A), their eyes would be centered (aligning with the dotted black line representing the center of the hallway), but the right portion of their body would collide with the wall. Since the eyes are to the left of the center of the PPO system, the eyes ought to be closer to the left wall than the right wall to ensure that the body at large is steered down the center (Figure 2-B).

Figure 2

Steering an Asymmetrical Person-Plus-Object System Through a Corridor

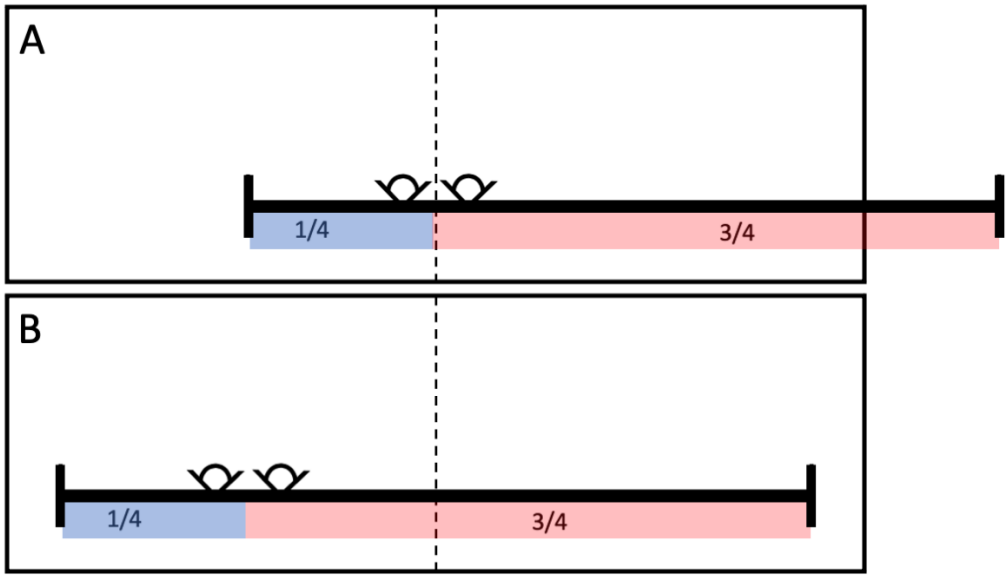

Note. Black dotted line represents the true center of the left and right boundaries (walls). A) Equalizing optic flow to the left and right fields of view results in the eyes being centered, but the PPO system colliding with the right wall. B) Overall PPO system is centered within the boundaries, even though the eyes are not centered.

A control law for steering an asymmetrical body would equate the speed of optic flow on the left and right sides of the focus of expansion *while also taking into account the proportion and size of the body extending from the midpoint of the eyes in each direction.* That is, it must account for the fact that one side of optic flow ought to be faster because the eyes will be closer to one side when the entire body is centered in the corridor. The generalized control law, accounting for asymmetrical bodies, is described in Equation 2.

Equation 2

Generalized Optic Flow Equalization Control Law Accounting for System Asymmetry

$$\Delta(\mathrm{F_L} - \mathrm{F_R}) = \mathrm{k}\,(v_r - v_l) + \left(\frac{w(p_r - p_l)}{2}\right), \text{ where}$$

F is the amount of force applied in each direction, resulting in lateral translations

k is an optical scaling coefficient

v is the horizontal angular velocity of optical flow

w is the total frontal width of the person-plus-object system

p is the proportion of w protruding from the point of observation (mean position of 2 eyes)

The generalized control law has two components. The first component specifies the actor's lateral position as a function of equalizing the optic flow on the left and right

field of view; This component is the same as the original control law. The second component then identifies the midpoint of the asymmetrical body and computes the direction and amplitude, in units of the frontal width of the body, of lateral adjustment required to place the midpoint of the asymmetrical body at the point of observation determined by the first component. In other words, the first component of the generalized control law places the eyes at the true center point of the environment. Then, the second component applies an adjustment so that the midpoint of the body – instead of the eye – is positioned at the previously determined center point.

Continuing with the above example (.25L/.75R asymmetry), let's assume that the total frontal width of the asymmetrical body is 1 m, and solve the second component of the generalized control law.

$$\Delta(\mathrm{F_L} - \mathrm{F_R}) = \mathrm{k}\,(v_r - v_l) + \left(\frac{w(p_r - p_l)}{2}\right)$$

$$\Delta(\mathrm{F_L} - \mathrm{F_R}) = \mathrm{k}\,(v_r - v_l) + \left(\frac{1(.75 - .25)}{2}\right)$$

$$\Delta(\mathrm{F_L} - \mathrm{F_R}) = \mathrm{k}\,(v_r - v_l) + \left(\frac{1(.5)}{2}\right)$$

$$\Delta(\mathrm{F_L} - \mathrm{F_R}) = \mathrm{k}\,(v_r - v_l) + (.25)$$

Therefore, the asymmetrical body is centered (and no lateral adjustments needed) when the eyes are positioned .25 m to the left of the position in which optic flow was equalized.

Importantly, this altered control law is also sufficient to guide locomotion when the body *is* symmetrical. Indeed, if the proportions of the body to the left and right of the eyes are equal (.5R/.5L), this control law replicates that of the original flow equalization

law used by Duchon & Warren (2002). In the case of a symmetrical body, the second component of the generalized control law will reduce to an adjustment of 0. To our knowledge, this alteration to the steering control law has yet to be empirically tested.

Purpose and Goals

The present experiments will build upon previous research to assess how a continuum of person-plus-object asymmetries impact optic flow equalization control laws for aperture passability and steering. To manipulate PPO asymmetry, participants will hold a 1m long horizontal bar with varying levels of asymmetry (70L/30R, 60L/40R, 50L/50R, 40L/60R, and 30L/70R).

The goal of Experiment 1 is to empirically test the altered optic flow equalization formula described in Equation 2. Participants holding asymmetrical bars will be placed in a virtual hallway with moving walls and will be asked to center themselves in the hallway, replicating Duchon & Warren (2002). By comparing the participants' placement in the hallway to the locations predicted by the altered optic flow equalization formulas, we aim to better understand the efficacy of the generalized control law and identify moderators of the centering performance.

The goal of Experiment 2 is to understand how the generalized control law can be applied to real world scenarios, like passing through doorways. Participants holding asymmetrical bars will pass through doors of various widths while their PPO system is tracked in space. The main dependent variable of interest is the participants' centering behavior when passing through the aperture, but additional exploratory variables will

provide rich information about the participants' shoulder turning behaviors and their likelihood of colliding with the aperture.

In both experiments, we hypothesize that participants will use the generalized control law equation (Equation 2) in order to center their person-plus-object systems in the virtual hallway (Experiment 1) and when passing through the aperture (Experiment 2). When measuring the midpoint of the participant's body, we expect to see a main effect of the wall speed condition as well as a main effect of the bar configuration. When measuring the midpoint of the overall person-plus-object system, we expect the main effect of bar configuration to be attenuated. That is, if participants are utilizing the generalized control law, they should successfully place the overall system in the middle of the virtual hallway or aperture, regardless of the level of bar asymmetry. Together, these experiments aim to better understand how the human perceptual systems utilize optical information to guide locomotion through the environment when external tool use generates uniquely altered body states.

CHAPTER II

Experiment 1

Method

Participants

Twenty-nine Clemson University undergraduate students (18 females, age M = 18.6, SD = 0.91, years of driving experience $M = 2.9$, SD = 1.06) participated in the study for partial course credit. All participants had normal or corrected-to-normal visual acuity and stereoacuity, no history of seizures, epilepsy, or neurological problems, and no motor impairments.

Simulation studies investigating the power of Hierarchical Linear Models suggest that the number of participants and the number of trials are both important for establishing sufficient power (Hofmann, 1997). To determine the Level 2 sample size (number of participants), a power analysis using Cohen's medium effect size of 0.3 (Cohen et al., 2003) and an alpha of 0.05 revealed that a sample size of 25 participants will produce power above 0.95.

To determine the Level 1 sample size (number of trials), the nested-ness of the data must be taken into account. Data from each trial will be nested within participants, such that some of the within-participant variance will be accounted for by between-subject variables. In this case, the number of trials is not an accurate representation of the number of independent observations.

The Intra-Class Correlation (ICC) is an index of nesting and can be used to adjust the number of trials so that it represents the effective sample size of independent

observations (Bickel, 2007). Using this adjustment with an ICC ranging from 0.25 to 0.35, 45 trials per participant would produce an effective total sample size ranging from 111 to 153. Power analyses using Cohen's medium effect size of 0.3 and an alpha of 0.05 revealed that both effective sample sizes would produce power levels above 0.95. This is sufficient power to detect cross-level interactions (Maas & Hox, 2005).

Materials & Apparatus

Virtual Environment. Participants completed the experimental tasks in a virtual hallway consisting of two walls. The virtual hallway was 4 m wide, and each wall extended indefinitely above, below, and in front the participant's viewpoint. To ensure that participants relied on optic flow and not splay angle or other optical variables, the hallway did not have a visible or implicit floor. Following Duchon & Warren (2002), a high contrast random texture was applied to the right wall, and its mirror image was applied to the left wall. Thus, all parameters of the wall texture were held constant for both walls, but the specific elements of the wall texture never matched up in position across the two walls (see Figure 3 for the texture, and Figure 4 for the virtual hallway with texture applied to both walls). The virtual environment did not include virtual self-avatars, but the participants were holding a virtual horizontal bar that corresponded in size, shape, and position to the one they were holding in the real world. The participant's viewpoint in the virtual world matched their eye-height in the real world.

Figure 3

Sample of High Contrast Random Texture Applied to the Virtual Walls

Figure 4

Virtual Hallway from the Participant's Point of View

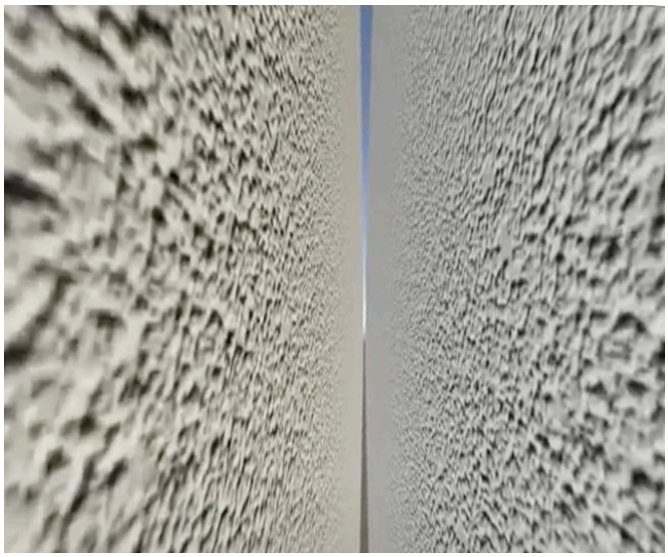

Participant's head movements and lateral movement, as well as the position of the bar in the real world were tracked with the HTC Vive headset and trackers at 90Hz, and this information was used to update the image displayed in the HMD so that the head and bar movements were consistent with participants' movements in the real world. The virtual environment was displayed using a HTC VIVE head mounted display (HMD), with a combined resolution of 2160 x 1200 pixels, a 90 Hz refresh rate, and a 110-degree horizontal field of view.

Horizontal Bar. In order to manipulate the symmetry of the person-plus-object system, participants held a horizontal bar on each trial. The bar was constructed from PVC pipe (2 cm radius), and consisted of a center piece with handle bars for the participant to hold and two side attachments. The center piece consisted of a 40 cm PVC pipe with T-sockets at each end. Extending from the T-sockets perpendicularly were two 30 cm pipe segments that served as handles for the participant. Side attachments were connected to the center piece via the T-sockets. The length of the side attachments differed based on the bar configuration condition such that the bar extending to the left of the center point was 30, 40, 50, 60 or 70 cm, and the bar extending to the right of the center point was 70, 60, 50, 40, or 30 cm, respectively. Across all conditions, the total length of the bar remained at 100 cm. Two HTC Vive trackers were affixed to the center piece of the bar (see Figure 5).

Because participants wore a head-mounted display for the duration of the experiment, the physical bar was not visible to participants. Instead, an identical virtual bar was modeled in Blender and inserted into the virtual environment, so that participants

saw a bar in the virtual world that corresponded to the bar they were holding in the real world. The virtual bar matched the size, shape, symmetry, and position of the physical bar, and was visible in the virtual space for the duration of each trial. To provide feedback to participants about whether or not the bar collided with the walls of the hallway, the last 2 inches of the virtual bar on the left and right were colored red. If the virtual bar collided with the virtual wall, the red tip on the side of the bar that collided with the wall would disappear due to being occluded by the virtual wall.

Stimuli

To simulate self movement in the virtual environment, each wall moved longitudinally toward the stationary participant at a constant velocity. Following Duchon & Warren (2002), the speed of each wall was determined by the wall speed condition. In the 1:1 condition, both walls moved at the same speed; in the 1:2 and 2:1 condition, one of the moved at twice the speed of the other wall. See Table 1 for details about the wall speed conditions. Notably, the speed of the each wall remained a constant velocity for the entirety of each trial to reduce the likelihood of VR sickness.

Table 1

Wall Speeds for the Right and Left Wall According to the Wall Speed Condition

Condition	Left wall	Right wall
1:1	2 m/s	2 m/s
1:2	2 m/s	4 m/s
2:1	4 m/s	2 m/s

Figure 5

Configuration of the Bar from PVC Pipe and T-sockets

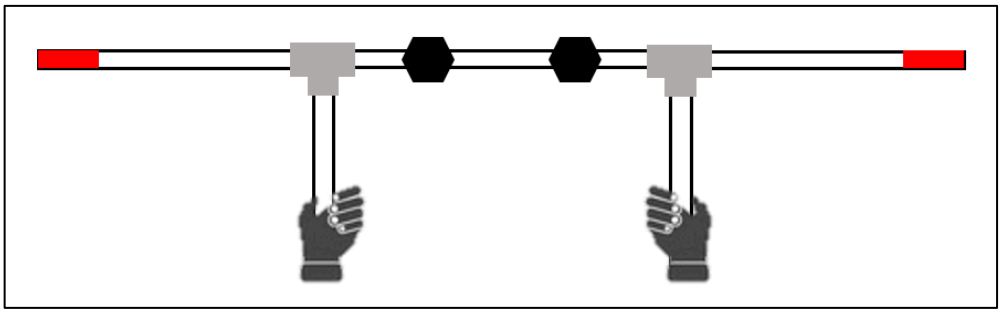

Note. Participants held the bar in front of their bodies, with their elbows bent at a 90 degree angle. This figure displays the 50L/50R symmetry configuration. The black hexagons denote the placement of the motion tracking pucks. Attachment pieces to the left and right of the center piece differed in length according to the bar configuration condition. In the real world, the bar remained all white. In the virtual environment of Experiment 1, the tips of the virtual bar were colored red to provide participants with visual feedback if the bar collided with the walls of the virtual hallway.

Procedure

After giving informed consent, participants completed a visual acuity and stereo-acuity test. Participants were administered the Stereo Fly Test (Stereo Optical, Chicago, IL), which tests gross stereopsis and fine depth perception. Participants were then instructed to measure their inter-pupillary distance (IPD) to help ensure the VIVE VR headset was properly adjusted to each participant. As detailed by Willemsen et al. (2008), the IPD test calls for participants to look into a mirror from a set distance and mark the location of each pupil in the mirror, then measure the distance between the two marks. The measured IPD was then used to set the inter-ocular distance on the VR headset

accordingly. By ensuring that the IPD of the VR headset is adjusted correctly for each participant, retinal disparity and vergence remained unchanged when participants were viewing the virtual environment.

The experimenter introduced participants to the bar and instructed them to hold the bar in front of their torsos using the designated handles, with their arms at their sides and their elbows bent to a 90 degree angle for the duration of the experiment. The experimenter then asked the participant to don the HMD and ensure it was fitted properly. Upon entering the virtual environment, participants saw the virtual hallway with non-moving walls and were handed the bar.

During a brief acclimation phase, participants were asked to complete a series of tasks that required them to interact with the bar and the environment. The purpose of this phase was to encourage participants to move (take lateral steps) naturally within the virtual environment while wearing the HMD, and to associate their virtual bar with the real world bar.

Once participants were comfortable with the virtual environment, they were given task instructions for the experiment. Participants were told that on each trial, they will be holding the horizontal bar, and will be placed at a random location in the virtual hallway. Participants were told that they would never be walking forward through the hallway; Instead, the walls of the virtual hallway moved toward the participant to simulate self-motion. Replicating Duchon & Warren (2002), participants were instructed to "move laterally (take steps to the left or right) so that you and your bar are in the center of the hallway". Each trial lasted 15 seconds, and once participants moved to the center of the

corridor, they were asked to remain there, facing forward, until the end of the trial. After two practice trials in which participants experienced the 50L/50R bar configuration and the 1:1 wall speed condition, experimental trials began.

The experiment took place in 5 phases of 9 trials, for a total of 45 trials. A randomly selected bar configuration was used in each of the 5 phases. Within each phase, participants experienced each of the three wall speed conditions three times each in random order. At the start of each trial, participants were placed in a random lateral location of the virtual hallway (restricted to the middle 2 meters of the hallway), with a randomly selected wall speed condition. Participants then moved laterally to a location in the hallway so that their bars were in the perceived center of the corridor. After 15 seconds, an occlusion screen appeared in the HMD to signify the end of the trial. While participants waited for the next trial, the textured walls disappeared (revealing an empty virtual environment), and a virtual tile was placed in the virtual environment which corresponded to the center point of the physical lab space. Participants were asked to walk to the virtual tile and stand on top of it. Once participants returned to the middle of the lab space, the next trial began. In between blocks, the HMD remained blank while the experimenter changed the side extensions of the physical bar to correspond with a different bar configuration.

After all experimental trials were completed, the experimenter assisted the participant in safely removing the HMD, and participants were administered the simulator sickness questionnaire (Kennedy, et al, 1993) followed by a demographics questionnaire including questions about the participant's driving experience (Machado-

León et al., 2016). The experimenter then debriefed, thanked, and dismissed the participant. The entire experiment lasted approximately 30 minutes.

Results

Data Preparation

Data Extraction. Raw data were collected such that each experimental session produced two .csv files. The first contained X (lateral), Y (vertical), and Z (longitudinal) positional data for the HMD and the left and right trackers placed on the bar, collected continually for the duration of the session. The second file contained trial level data, including the phase, bar configuration, and wall-speed condition for each individual trial.

A data-extraction program was written in Python 3.7 (Python.org) that took each session's two .csv files as input, and returned 45 individual .csv files, each containing the motion tracking data for a single trial. These motion data files, parsed into individual trials, were then submitted to additional scripts to filter the data and compute centering variables.

To extract the final position of the participant on each trial, the lateral position of the participant's HMD was averaged across all data points in the final 5 seconds of each trial. To extract the final position of the midpoint of the bar on each trial, the lateral position of the bar was averaged across all data points in the final 5 seconds of each trial. Since the trackers affixed to the bar did not correspond to the midpoint of the bar for all bar configurations, the midpoint of the bar was computed by taking the lateral position of one bar tracker and adding a known displacement value based on the bar configuration. For example, if the bar extended 70 cm to the left of the tracker and 30 cm to the right of

the tracker, then the midpoint of the bar can be calculated as 20 cm to the left of the location of the tracker. Position values range from -200 cm (representing the left wall) to 200 cm (representing the right wall). A positional value of 0 represents the true midpoint of the virtual hallway.

Data Filtering. To reduce components of noise in the final signal, each trial's motion tracking data were submitted to a filtering process. As suggested by (Winter, 2005), biomechanical movement data with a fundamental frequency of 1Hz were subjected to a low-pass Butterworth filter normalized with respect to a cutoff frequency of 6Hz. This filter resulted in a 90 degree phase lag, so the same filter was run in the reverse direction of time to return the filtered data to be in phase with the raw data. The full filtering process was written and completed within a Python program.

Hierarchical Linear Modeling

Overview. Due to the use of repeated measures, data from this experiment is nested within each participant, creating multiple levels of variance. In a typical mixed model regression, some variance is due to within-participant variables, and some variance is due to between-participant variables. In the present within-subjects experiment, data were nested into 3 levels: trials (Level 1) are nested within phases (Level 2), which are nested within participants (Level 3), as demonstrated in Figure 6. The Intra-Class Correlation (ICC) is a metric of model nestedness which quantifies the proportion of total variance that occurs at the between-subjects level (Level 2). Across all analyses, the average ICC was 0.32, which suggests that an average of 32% of total variance was between-participant variance. In order to properly account for variance at each level of

data, Hierarchical Linear Modeling (HLM) was used (Hofmann, 1997; Woltmann et al., 2012).

Figure 6

3-Level Model of Nested Variance

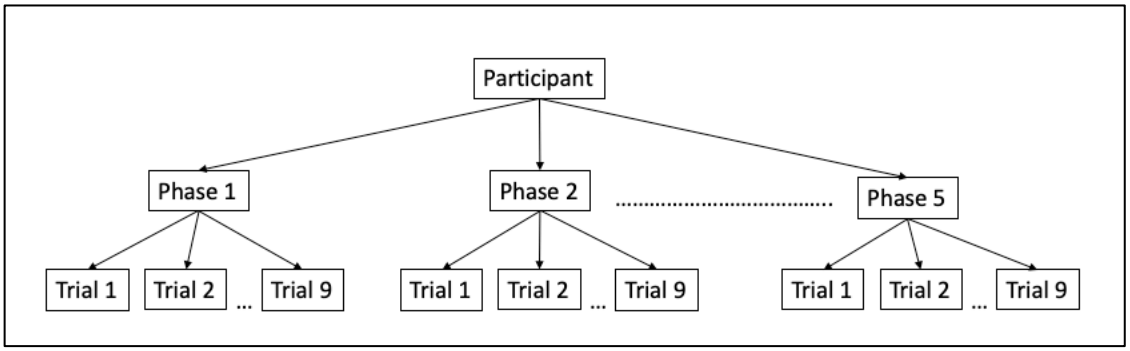

In a mixed model regression, level 1 variables (i.e., wall speed condition, trial) produce residual variance, and the regression coefficient (*B*) can be interpreted as: *a 1-unit increase in [level 1 variable] results in a B-unit increase in [dependent variable].* Level 2 (i.e., bar configuration) and level 3 (i.e., driving experience) variables produce intercept variance, and the regression coefficient (*B*) can be interpreted as: *a 1-unit increase in [level 2 or 3 variable] results in a B-unit increase in the intercept of the regression equation.* Cross-level interactions produce slope variance, and can be interpreted as the differences in level 1 slope coefficients across different level 2 or level 3 groupings.

When using HLM, it is important to hold the regression coefficient of the intercept constant across all models. In order to do this, all continuous independent

variables were grand-mean centered. As a result, the intercept coefficient of the regression equation represents the predicted outcome when all continuous variables are held at their average.

A conservative model was implemented to minimize the likelihood of spurious results from the analyses. For each analysis, an initial main effects model was run, such that all main effects (Level 1 and Level 2) were included in the analysis at once. Results for all main effects are presented from this model. Next, to analyze interaction effects, individual interaction terms were added to the main effects model, one at a time. In other words, interaction A was included with the main effects model to gather results for interaction A, then interaction A was removed from the model. Next, interaction B was added to the main effects model, and so on. Results of each interaction are reported from the model in which that interaction was included. For 3-way interactions, the model also included all two-way interactions that built up to the 3-way interaction.

Effect sizes. Effect sizes for each fixed effect will be presented as the change in R^2 (proportion of explained variance) comparing the model that includes the fixed effect and that same model with the effect removed. The resulting sr^2 can be interpreted as the percentage of variance accounted for by the fixed effect.

Outlier analysis. For each analysis, residuals were obtained from the full model, and then standardized. The standardized residuals were plotted and then inspected for overly influential cases that fell outside of a normal distribution (Cohen et al., 2003). Selected outliers were removed from the dataset. In all analyses, fewer than 1% of trials were removed due to outliers.

Predicting Centering Behavior

Midpoint of the Body. A hierarchical linear model was used to assess the effects of Trial, Wall Speed, and Bar Configuration on the participants' body midpoint at the end of each trial. As a reminder, a positional value of 0 represents the true center of the hallway, with positive values representing positions to the right of center and negative values representing positions to the left of center. See Table 2 and Table 3 for results of the model. Holding all variables at their average (Wall Speed = 1:1, bar configuration = 50L/50R), participants' body midpoints were positioned 2.42 cm to the right of the true midpoint of the hallway. Thus, on average the participants centered their bodies so that they were at a location very close to the hallway's center (i.e., the midpoint of the hallway is denoted by a position of 0).

There was main effect of Wall Speed which accounted for 31% of the residual variance. Post-hoc Bonferroni-corrected t-tests revealed that participants moved their bodies away from the faster moving wall. Compared to the 1:1 wall speed condition (M = 2.53, SD = 2.8), the midpoint of the participants bodies shifted significantly to the right when the left wall was moving faster (2:1 wall speed condition: M = 20.70, SD = 2.7, $t(1258) = 14.77$, $p < 0.001$). Similarly, compared to the 1:1 wall speed condition, participants shifted their bodies significantly to the left when the right wall was moving faster (1:2 wall speed condition: M = -15.65, SD = 2.8, $t(1258) = 14.67$, $p < 0.001$).

Further, there was a significant main effect of the Bar Configuration, which accounted for 25% of the intercept variance. As the bar configuration changed incrementally from 70L/30R to 60L/40R to 50L/50R and so on, the midpoint of

participant's bodies moved 9.4 cm leftward. In other words, participants shifted their bodies in accordance with the bar configuration to ensure that the center of the bar remained in a constant position.

Table 2

Omnibus F Test Results for Fixed Effects Predicting the Midpoint of the Body in Experiment 1

Predictor	F	df1	df2	sig	sr^2
Trial	0.072	1	1258	0.79	--
Wall Speed	430.67	2	1258	<0.001	0.31
Bar Configuration	693.05	1	1258	<0.001	0.25
Driving Experience	0.35	1	27	0.56	--
Trial * Wall Speed	1.19	2	1256	0.3	--
Trial * Bar Configuration	3.17	1	1275	0.08	--
Wall Speed * Bar Config	0.27	2	1256	0.76	--
Trial * Wall Speed * Bar Config	1.34	2	1251	0.26	--

Table 3

Regression Coefficients for Fixed Effects Predicting the Midpoint of the Body in Experiment 1

Predictor	B	SE	df	t
Intercept	2.36	2.97	29	0.79
Trial	-0.01	0.04	1258	-0.27
Bar Configuration	-9.4	0.36	1258	-26.32^{***}
Driving Experience	0.31	0.51	1258	0.59
Trial * Bar Configuration	-.06	0.03	1275	-1.78

Note. *** denotes p < .001, ** denotes p < .01, * denotes p < .05

Importantly, the amplitude of the shift in body position was nearly identical to the shift in the midpoint of the bar across each bar configuration (e.g., as the bar configuration shifted from 50L/50R to 40L/60R, the midpoint of the bar shifted 10 cm to the right, and participants' bodies shifted 9.4 cm to the left). The main effects of wall speed and bar configuration are displayed in Figure 7. There were no other significant main effects or interactions in the model.

Figure 7

Position of the Midpoint of the Body by Wall Speed and Bar Configuration

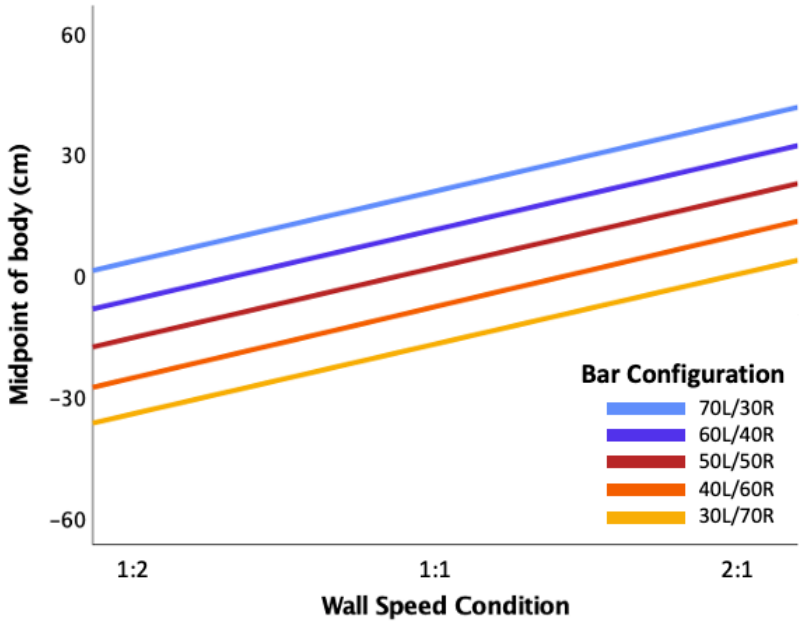

Note. A midpoint position of 0 cm represents the true center of the hallway, positive values are to the right of center, and negative values are to the left of center.

Midpoint of the Bar. To assess the effects of trial, wall speed, and bar configuration on the position of the midpoint of the bar in the hallway, a second

hierarchical linear model was run. See Table 4 for results of the omnibus F test and Table ***5*** for regression coefficients for continuous predictors.

Table 4

Omnibus F Test Results for Fixed Effects Predicting the Midpoint of the Bar in Experiment 1

Predictor	F	df1	df2	sig	sr^2
Trial	0.202	1	1255	0.65	--
Wall Speed	457.37	2	1255	<0.001	0.42
Bar Configuration	1.08	1	1255	0.29	--
Driving Experience	0.79	1	27	0.38	--
Trial * Wall Speed	1.03	2	1253	0.36	--
Trial * Bar configuration	0.01	1	1272	0.99	--
Wall Speed * Bar Configuration	0.11	2	1253	0.89	--
Trial * Wall Speed * Bar Configuration	1.29	2	1248	0.28	--

Table 5

Regression Coefficients for Fixed Effects Predicting the Midpoint of the Bar in Experiment 1

Predictor	B	SE	df	t
Intercept	2.42	2.93	29	0.82
Trial	.02	0.094	1255	-.45
Bar Configuration	-.36	0.35	1255	-1.04
Driving Experience	0.45	0.5	1255	0.89
Trial*Bar Configuration	-.0003	0.03	1272	-.01

Note. *** denotes p < .001, ** denotes p < .01, * denotes p < .05

Holding all variables at their average (Wall Speed = 1:1, bar configuration = 50L/50R), participants positioned the midpoint of the bar 2.42 cm to the right of the true midpoint of the hallway. This position overlaps closely with the average midpoint of

body when holding all variables at their average, since the midpoint of the 50L/50R bar is in line with the midpoint of the participant's body.

There was a significant main effect of wall speed, accounting for 42% of the residual variance. Post-hoc Bonferroni-corrected t-tests revealed that participants moved the midpoint of the bar away from the faster moving wall. Compared to the 1:1 wall speed condition (M = 2.05, SD = 2.8), the midpoint of the bar shifted significantly to the right when the left wall was moving faster (2:1 wall speed condition: M = 20.53, SD = 2.8, $t(1255) = 14.98$, $p < 0.001$). Similarly, compared to the 1:1 wall speed condition, participants shifted the midpoint of the bar significantly to the left when the right wall was moving faster (1:2 wall speed condition: M = -16.08, SD = 2.9, $t(1255) = 15.40$, $p < 0.001$).

There were no other significant predictors of the midpoint of the bar. While there was a significant main effect of bar configuration on the position of participant's bodies, the effect of bar configuration was eliminated when predicting the position of the midpoint of the bar. This is reflected in Figure 8 as the overlapping of lines corresponding to each bar configuration.

Testing the Altered Control Law

The generalized control law (Equation 2) was used to calculate the balance point (expected midpoint of the body) for each combination of wall speed and bar configuration. The resulting balance point was the sum of two components: the balance point determined by equating the angular velocity of optic flow on the left and right sides of the visual field ($w_r - w_l$), and the lateral translation required to account for the level

of asymmetry in the person-plus-object system $\left(\frac{l(p_r - p_l)}{2}\right)$. The optic flow component revealed that the balance point for the 1:2 wall speed condition was 66 cm from the center, away from the faster moving wall, and that the lateral translation due to the PPO asymmetry changed in increments of 10 cm (e.g., the 40L/60R bar configuration required a lateral translation of 10 cm to the left, the 30L/70R bar configuration required a lateral translation of 20 cm to the left). To determine their individual contributions to participants' centering behavior, these components were included separately into a regression model predicting the lateral position of the midpoint of the body. See Table 6 for results of the regression model.

Figure 8

Position of the Midpoint of the Bar by Wall Speed and Bar Configuration

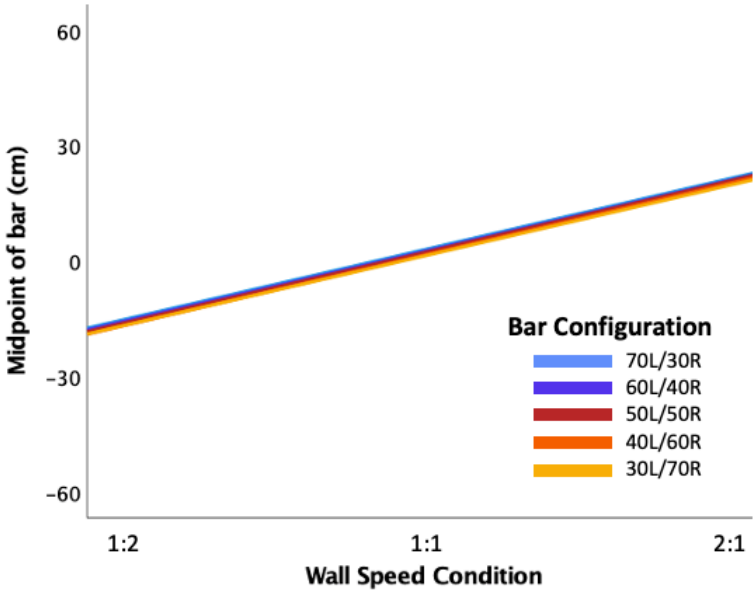

Note. A midpoint position of 0 cm represents the true center of the hallway, positive values are to the right of center, and negative values are to the left of center.

Table 6

Regression Coefficients for Fixed Effects Predicting the Midpoint of the Bar From the Generalized Control Law

Predictor	B	SE	df	t ($H_0 = 0$)	t ($H_0 = 1$)	sr^2
Intercept	2.48	2.72	28	0.91	--	--
Optic flow equalization component	0.28	0.01	1260	29.37^{***}	72^{***}	0.31
PPO asymmetry component	0.94	0.04	1260	21.42^{***}	1.5	0.24

Note. *** denotes $p < .001$, ** denotes $p < .01$, * denotes $p < .05$.

In general, participants positioned their body midpoint in the direction predicted by the altered control law, but only travelled a portion of the predicted distance. Both components were significant predictors of the body midpoint, but the PPO asymmetry component had a much larger effect. For reference, if participants' behaviors followed the altered control law *exactly*, the slope coefficients for both components would equal 1. The effect of the PPO asymmetry component ($B = 0.94$) was not significantly different from the ideal slope value of 1, while the effect of the optic flow equalization component ($B = 0.28$) was significantly lower than a slope value of 1. This is reflected in Figure 9: within each wall speed condition, the data points produce a slope of approximately 1, while the trend across wall speed conditions produces a smaller change than expected.

Participants' behavior from this experiment is better explained using a weighted version of the generalized control law, such that each component of the equation has a multiplicative weighting commensurate with its impact on the participant's behavior. The weighted generalized control law is represented in Equation 3, with relative weightings in bold. Figure 10 shows the body midpoint data plotted against the positions predicted by

the weighted generalized control law. The resulting regression line has an intercept at 0 and a slope of 1, and the weighted generalized control law accounts for over 50% of the variance in the body midpoint position.

Equation 3

Weighted Generalized Optic Flow Equalization Control Law

$$\Delta(\mathrm{F_L} - \mathrm{F_R}) = \mathrm{k}\,\{\mathbf{0.28}(v_r - v_l)\} + \mathbf{0.94}\left(\frac{w(p_r - p_l)}{2}\right), \text{ where}$$

F is the amount of force applied in each direction, resulting in lateral translations

k is an optical scaling coefficient

v is the horizontal angular velocity of optical flow

w is the total frontal width of the person-plus-object system

p is the proportion of w protruding from the point of observation (mean position of 2 eyes)

Figure 9

Average Midpoint of the Body Plotted Against the Midpoint Determined by the Generalized Control Law (Equation 2)

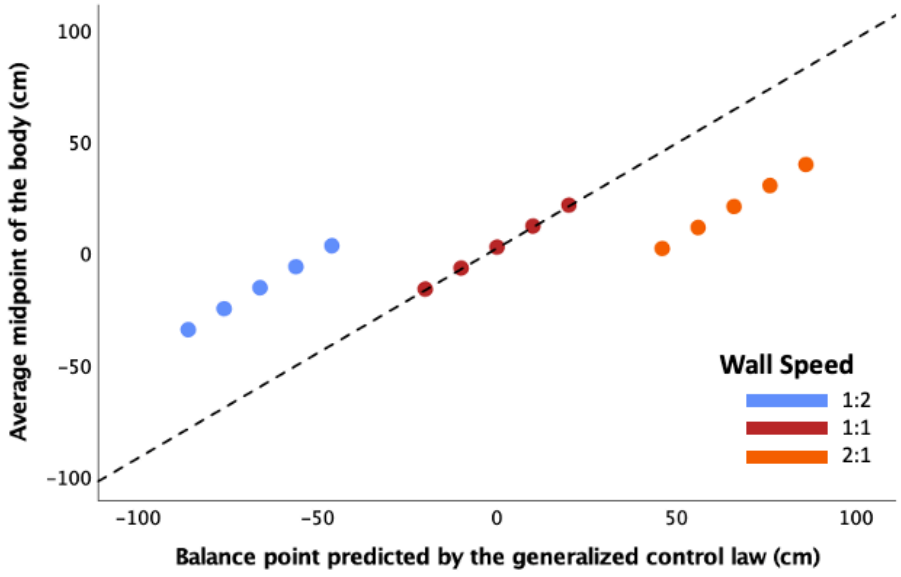

Note. Data points represent the average midpoint of the body for each wall speed condition * bar configuration averaged across all participants. The dotted black line represents the expected position of the average body midpoint, as determined by the generalized control law. A midpoint position of 0 cm represents the true center of the hallway, positive values are to the right of center, and negative values are to the left of center. Wall speed conditions are indicated by colored data points; Bar configurations are indicated by incremental increases within each color.

Figure 10

Position of the Midpoint of the Body Plotted Against the Positions Predicted by the Weighted Generalized Control Law (Equation 3)

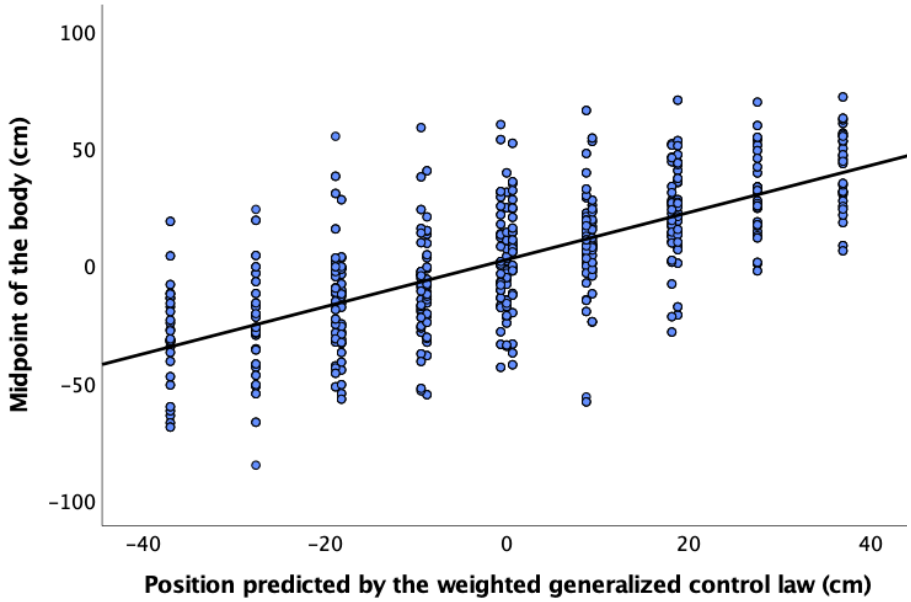

Note. Data points represent the average midpoint of the body for each wall speed condition * bar configuration, calculated separately for each participant. A midpoint position of 0 cm represents the true center of the hallway, positive values are to the right of center, and negative values are to the left of center. The best fit line has an intercept of 0 and a slope of 1.

Discussion

The goal of Experiment 1 was to understand if humans can successfully center an asymmetrical person-plus-object system within a moving hallway utilizing the generalized optic flow equalization control law described in Equation 2. The control law is broken into two components: 1) the equalization of optic flow in the left and right fields of view, and 2) the lateral adjustment accounting for the asymmetry of the PPO system. Both components were tested separately, such that changes to the wall speed

manipulated optic flow speeds (resulting in positional changes predicted by the first component of the control law), and changes to the bar configuration manipulated the symmetry of the person-plus-object system (resulting in position changes predicted by the second component of the control law).

Results indicate that participants did rely on the optic flow equalization component when centering themselves in the moving hallway. When the walls moved at the same speed (1:1 condition), participants positioned themselves very close to the center of the hallway, as indicated by the regression intercept being not significantly different from zero (recall that a zero position represents the true center of the hallway). When one wall moved at twice the speed of the other wall (1:2 and 2:1 conditions), participants consistently moved away from the faster moving wall. This finding replicates previous research showing that humans use optic flow equalization strategies to guide centered steering (Chou et al., 2009; Duchon & Warren, 2002; Kountouriotis et al., 2013). Further, this work suggests that the optic flow equalization strategy is used in the context of a high fidelity immersive virtual environment.

It is important to note that while participants moved in the direction specified by the optic flow equalization strategy (away from the faster moving wall), they failed to travel the full magnitude of the distance predicted by the control law. According to the optic flow equalization component of Equation 2, participants should have traveled 66 cm from the center of the hallway when in the 1:2 and 2:1 wall speed conditions. Results showed that participants positioned themselves an average of 18 cm from the center of the hallway, which is about 28% of the predicted magnitude. For reference, Duchon &

Warren (2002) found that participants in a walking task moved about 65% of the predicted magnitude. The reduced effect in the current experiment could be due to factors associated with using an immersive virtual environment projected into a head-mounted display.

While Duchon & Warren (2002) used a large projection screen and a head-mounted mask that reduced horizontal field of view to 90°, the current experiment used a head-mounted display with a larger horizontal field of view (110°) within an immersive virtual environment that allowed participants to turn their heads to see the virtual environment above, below, and beside them. One possible reason that participants did not move as far as expected could be due to the compression of depth caused by head-mounted displays, resulting in an underestimation of perceived distance (Armbrüster et al., 2008; Geuss et al., 2012; Loomis & Knapp, 2003; Wann et al., 1995). If participants perceived the walls to be closer than they actually were, then they may have been less likely to move large distances within the hallway to reduce their likelihood of the bar colliding with the wall.

Another likely factor leading to the reduced magnitude of lateral movement was the participant's ability to shift their direction of gaze via head and eye rotations. Rotation of the eyes, head, and body can result in shifts of the participant's fixation point and visual field. Since the optic flow equalization strategy calls for a matching of flow speeds in the left and right visual fields, any shifts in the visual field could impact the participants' ability to extract (detect) and scale the optical information as described in the control law. Indeed, head rotations have been shown to impact an actor's ability to

use optical variables to extract their direction of heading (J. J. Gibson, 1950; Li & Chen, 2010; Li & Warren, 2000; Regan & Beverley, 1982), and would also inherently impact the portions of the optic flow field that are available for detection and equalization. Since participants in the current study were concerned with the position of the tips of the horizontal bar in relation to the walls of the hallway, most participants engaged in at least some rotation of the head about the yaw axis. The head rotations may have been exacerbated by the limited field of view in the headset, which made it impossible for participants to view the entire length of the bar without shifting their direction of gaze by turning their heads, especially for the asymmetrical bar configurations. This highlights the fact that the equalization control law is most effective when the direction of gaze is aligned with the direction of heading, such that the focus of expansion is in the center of the visual field.

To illustrate the impact of head rotation on one's ability to detect and equalize optic flow information across the left and right visual field, consider the example in Figure 11. The horizontal angular velocity of optic flow is calculated as the portion of field of view (degrees) that an object travels across over a unit of time. In Figure 11-A, a schematic eye is placed in a hallway, and stimuli (stars) on each wall travel towards the eye at equal velocity. The visual field, with a 210 degree horizontal field of view, is dissected along the direction of gaze into a left and right side, which is indicated by the colored shading. Drawing lines from the eye to the stimuli at time 1 and time 2 produces an angle on each side of the field of view, denoted as V_L and V_R. Research suggests that actors engaging in flow equalization strategies are sampling optic flow speeds from

lateral portions of the optic array that are either perpendicular to the direction of gaze (Duchon & Warren, 2002), or perpendicular to the direction of travel (Srinivasan et al., 1991). In the case of Figure 11-A, because the direction of gaze is aligned with the direction of heading, the portions of the optic array perpendicular to each are the same. Because the angle produced on the right is larger than that of the left, this indicates a faster flow speed on the right, requiring a positional shift to the left in order to equalize the flow speeds.

Figure 11-B and Figure 11-C illustrate optic flow sampling when the head and/or eyes are rotated such that the direction of gaze no longer aligns with the direction of heading. If the schematic eye samples the optic array portions that are perpendicular to the direction of gaze (Figure 11-B), this results in a comparison of the speed of flow in front of the eye on the left and behind the eye on the right. The angular velocities sampled are nearly equal, suggesting (falsely) that the actor is in the center of the hallway and that no lateral translations are required. If the schematic eye samples the optic array portions that are perpendicular to the direction of heading (Figure 11-C), it will fail to detect an angular speed on the right side because this portion of the optic array is outside of the field of view. In both cases, rotation of the head reduces the effectiveness of the flow equalization strategy by limiting the extent to which the relevant portions of the optic array can be detected and scaled.

The use of an immersive virtual environment eliminates the ability to experimentally control the alignment of the focus of expansion within the participant's

field of view, which may have resulted in an attenuation of the use of optic flow equalization strategies. Future research should investigate the unique effects of head

Figure 11

Optic Array Detection During Rotation and Non-rotation

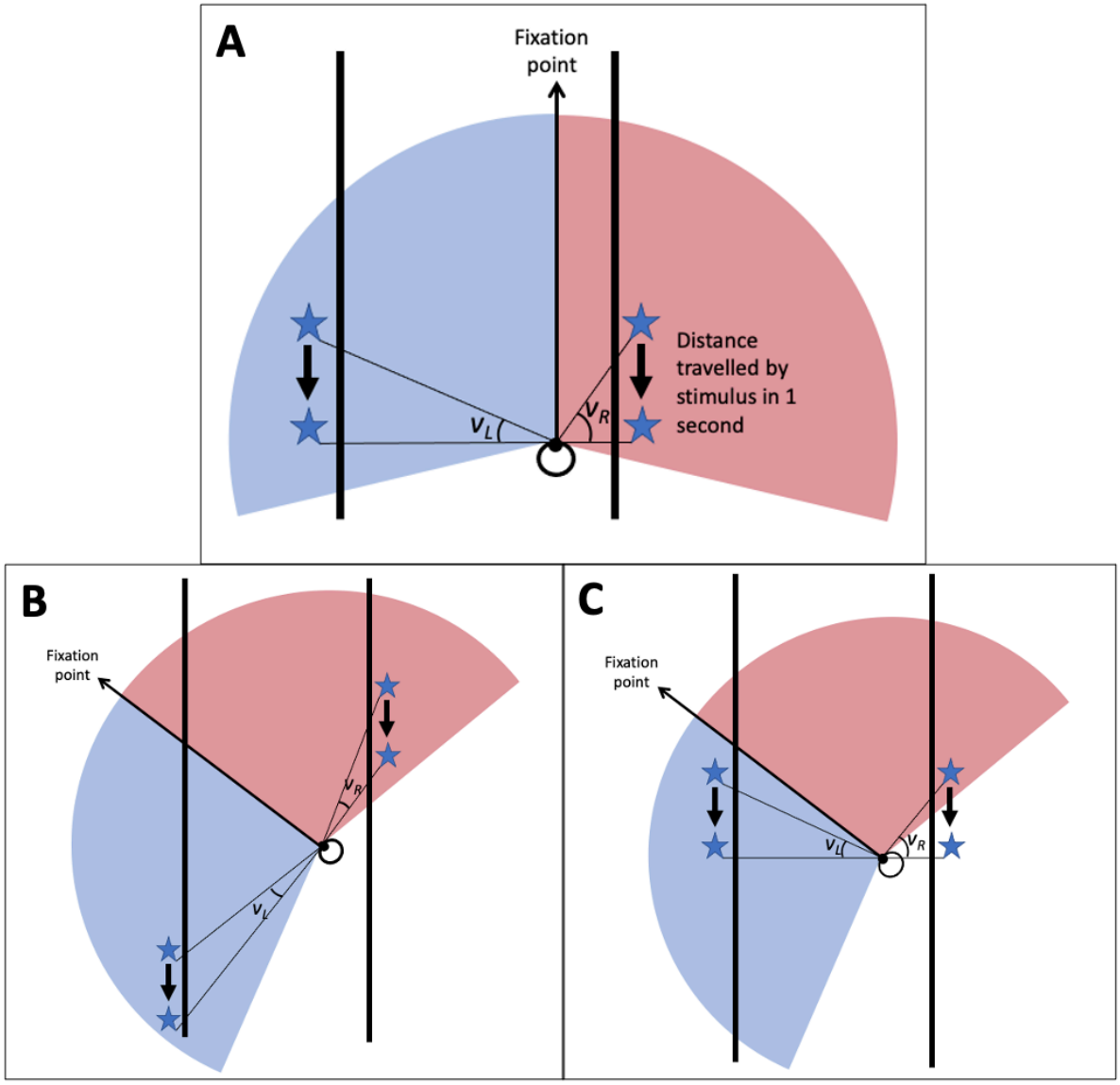

Note. A) Detecting optic flow speed on the left and right fields of view when the direction of gaze aligns with the direction of heading. B) Detecting optic flow speeds perpendicular to the direction of gaze when the head is rotated. C) Detecting optic flow speeds perpendicular to the direction of heading when the head is rotated.

rotation on the use of optic flow equalization strategies, and utilize head-mounted displays with larger fields of view.

Other possible reasons for the reduced magnitude of lateral position in the current experiment could be attributed to the use of other optical variables available in the virtual environment. In the current experiment, the height of each wall was extended above and below the participant's eye-height to a near-infinite length. This was done to eliminate splay angles when the participants were looking directly forward at eye height. However, if participants were to look directly up or down, they would be able to utilize the splay angle produced by the edge of the wall meeting the background of the virtual environment. Thus, participants could have been equalizing the left and right splay angles, resulting in an attenuation of the effect of optic flow (Duchon & Warren, 2002). With the ability to rotate their heads and see the walls at their sides, participants could have also been equalizing the average scale of the textures on each wall, another strategy that would possibly attenuate the effect of optic flow.

Due to space limitations within the lab, the experimental task asked participants to step left and right until they felt like they were in the center of the hallway. Participants may have been reluctant to travel too far left or right for fear of colliding with objects in the real environment, particularly because they could not see the physical space while wearing the HMD. This concern was accounted for by the acclimation period in which the experimenter allowed the participant to move the full width of the virtual hallway, but perhaps results would have been different in a larger space. It is also important to note

that in this experiment, the optic flow was not created by self-motion, but instead was passively imposed on a mostly stationary observer. That is, participants were not creating the optic flow by walking forward through the hallway. Thus, since it was simulated flow that was creating perceived motion, the natural perception-action linkage between the motor system and resulting optic flow was absent. This may have affected how, or to what degree, participants utilized optic flow information. Future research should utilize a more naturalistic task, such as asking participants to walk the length of the hallway.

Finally, the reduced effect of the wall speed manipulation relative to the asymmetry manipulation may have been due in part to the experimental design. The repeated-measures experiment was completed in phases such that participants received the same bar configuration for 9 trials in a row before switching to a different bar configuration. Within each phase, the wall-speed conditions changed randomly from trial to trial. This may have provided participants with a better opportunity to calibrate to the asymmetrical bar due to its repeated exposure, potentially resulting in a stronger effect of bar configuration. Future research could rule out this confound by designing a true random experiment, such that the bar configuration and wall speed condition are randomly assigned on each individual trial.

Results also show that humans accurately adjusted their lateral position to account for the asymmetry of the PPO system, following the asymmetrical PPO component of the generalized control law. In this case, participants shifted the position of their bodies in the correct direction *and* with the correct magnitude. For every 10 cm shift in the

midpoint of the bar (e.g., changing from the 50L/50R configuration to the 60L/40R configuration effectively shifts the midpoint of the bar 10 cm to the left), participants moved on average 9.4 cm toward the longer side of the bar. Compared to the effect of optic flow in which participants moved 28% of the predicted distance, participants moved 94% of the predicted distance for the effect of system asymmetry. This result is further confirmed by the nonsignificant effect of bar configuration when using the midpoint of the bar as the dependent variable. Figure 7 shows how participants shifted the midpoint of their *bodies* differently for each bar configuration, and this effect is completely eliminated when studying the midpoint of the *bar,* such that the midpoint of the bar was moved to the same position regardless of the bar configuration. As previously stated, the optic flow manipulation was decoupled from kinesthesis, and this may have impacted the extent to which participants utilized the flow information. On the other hand, the manipulation of asymmetry of a hand-held bar had a stronger coupling of perception (both visual and haptic) and action, which may have improved participants' ability to detect and accurately scale the asymmetry information.

This finding suggests that humans are capable of perceiving the length of the horizontal bar in terms of the amount of bar extending to the left and right of their body midpoint, and can shift the lateral position of their bodies accordingly. Humans have been shown to accurately perceive the length of handheld tools using both haptic and visual information. Haptically wielding an object that is occluded from view can support the accurate perception of the objects length and shape via the invariant inertia tensor about a rotating joint (Burton et al., 1990; Burton & Turvey, 1990; Pagano et al., 1993).

Further, when an object is held at an intermediate position along its length, research has shown that humans can perceive both the full length of the object as well as the partial length of the object extended to one side of the hand (Hajnal et al., 2007; Pagano et al., 1994; Palatinus et al., 2011; Wagman et al., 2017). Additionally, object length, as it relates to action capabilities, can be perceived visually in the absence of haptic information (Bhargava, 2020; Day et al., 2017; Wagman & Taylor, 2005). Participants in the current experiment were likely attuning to both sets of information to accurately perceive the length of the bar extending to the left and right of the midpoint.

Overall, Experiment 1 has shown that humans can accurately perceive the length and asymmetry of a PPO system and adjust the position of their bodies - beyond that of an optic flow equalization strategy alone - to account for the asymmetry during a hallway centering task. The generalized control law described in Equation 2 accounted for over 55% of the variance in participant's centering behaviors, compared to the 31% of variance accounted for by the original control law described in Equation 1. Since the generalized control law has been shown to be effective for steering an asymmetrical PPO, Experiment 2 will seek to understand if and how the control law is applied to a naturalistic task of passing through apertures.

CHAPTER III

Experiment 2

Method

Participants

Thirty Clemson University undergraduate students were recruited to participate in the study for partial course credit. All participants were screened to ensure normal or corrected-to-normal vision and no motor impairments. A power analysis using Cohen's medium effect size of 0.3 (Cohen et al., 2003) and an alpha of 0.05 revealed that a sample size of 30 participants will produce power above 0.95. Two participants were removed from the dataset due to malfunction of the data collection technology, resulting in a total of 28 participants (17 female, age $M = 18.5$, $SD = 0.75$, years of driving experience $M = 2.5$, $SD = 0.95$).

Materials & Apparatus

Room Setup and Aperture. The experiment was run in a 10 X 15 m room. A walking path extended 5 m in front of the aperture, and 2 m behind the aperture. The aperture was constructed of two 8 ft tall * 2 ft wide room partitions constructed from PVC pipe. Each partition was covered in black curtain. The left side of the aperture was fixed to the ground, while the right side was repositionable to create aperture widths between 85 – 145 cm. A yellow curtain was hung against the back wall 2 meters behind the aperture to remove any background visual information that may have helped participants estimate the width of the aperture (see Figure 12).

Figure 12

Aperture Constructed from Two PVC Pipe Room Partitions

Horizontal Bar. In order to manipulate the symmetry of the person-plus-object system, participants held a horizontal bar on each trial. This experiment used the same horizontal bar from Experiment 1, which was 1 meter in length. The asymmetry of the bar was manipulated to produce five bar configurations: 70L/30R, 60L/40R, 50L/50R, 40L/60R, and 30L/70R, see Figure 5.

Motion Tracking. The HTC Vive system (HTC, Taiwan) was used to collect the participants' positional data over time. Two HTC Vive Base Stations were mounted onto standard tripods and positioned 7 feet above the ground at a 45-degree angle in each corner of the room.

In order to acquire motion tracking data about the participant's body and the horizontal bar, multiple HTC Vive Trackers were used. Trackers were placed above each shoulder by securing trackers to a backpack's shoulder straps using screws and a 3D printed plastic insert. Two additional trackers were mounted to the center piece of the bar. Lastly, a single tracker was mounted to the fixed (i.e., right) column of the aperture. For each tracker, positional data along the X, Y, and Z axes were collected at a sampling rate of 90 Hz, then sent to a Dell computer through a SteamVR program.

Procedure

After giving informed consent, participants completed a short questionnaire to collect demographic information and information about each participants' driving experience (Machado-León et al., 2016). The participant was then fitted with an empty backpack, and the straps were adjusted so that the attached motion trackers rested directly on top of the participant's shoulders. The experimenter then introduced participants to the bar and instructed them to hold the bar in front of their torsos using the designated handles, with their arms at their sides and their elbows bent to a 90 degree angle for the duration of the experiment. In this way, the orientation of the bar was fixed to the orientation of the participant's shoulders.

For the experiment, participants performed an aperture passability task. On each trial, participants stood at the starting line 5 m away from the aperture while holding the horizontal bar, and were asked to close their eyes. Once the experimenter manually adjusted the width of the aperture, participants were asked to open their eyes, walk forward at a natural pace, and pass through the aperture without letting the bar hit the

sides of the aperture. Participants were informed that they could turn their shoulders (and the bar by extension) when passing through the door if they wished to do so. Once they passed through the door, participants walked along the outside of the aperture, returned to the starting line, and closed their eyes until the next trial began.

The experiment took place in 5 phases of 15 trials, for a total of 75 trials. A randomly selected bar configuration was used in each of the 5 phases. Within each phase, participants passed through five different aperture widths (85, 100, 115, 130, and 145 cm). Each aperture width was presented three times each in random order. In between phases, participants handed the bar to the experimenter, who then changed the side extensions of the bar to correspond with a different bar configuration. At the conclusion of all trials, the experimenter removed all equipment and debriefed the participant. Each session lasted approximately 45 minutes.

Results

Data Preparation

Data Extraction. Data extraction techniques were similar to that of Experiment 1. Raw data were collected such that each experimental session produced two .csv files. The first contained X (lateral), Y (vertical), and Z (longitudinal) positional data for each of the motion trackers placed on the left and right shoulders, the bar, and the right (fixed) side of the aperture), collected continually for the duration of the session. The second file contained trial level data, including the phase, bar configuration, aperture width, and start and stop times for each individual trial.

A data-extraction program was written in Python 3.7 (Python.org) that took each session's two .csv files as input, and returned 75 individual .csv files, each containing the motion tracking data for a single trial. These motion data files, parsed into individual trials, were then submitted to additional scripts to filter the data and compute centering variables.

Data Filtering. To reduce components of noise in the final signal, each trial's motion tracking data were submitted to a filtering process. Analysis of each data file revealed a maximum stride frequency of 1Hz (1 stride is 2 steps, so this is equivalent to 120 steps per minute). As suggested by (Winter, 2005), biomechanical movement data with a fundamental frequency of 1Hz was subjected to a low-pass Butterworth filter normalized with respect to a cutoff frequency of 6Hz. This filter resulted in a 90 degree phase lag, so the same filter was run in the reverse direction of time to return the filtered data to be in phase with the raw data. The full filtering process was written and completed within a Python program.

Computing Movement Variables. A Python script was written to compute a multitude of variables describing participants' aperture crossing behavior. For a full list of variables, see Table 7. On each trial, the first meter after the starting line was considered as a gait initiation period, and the corresponding motion tracking data were discarded. The sustained walking period consisted of the onset of sustained walking (1 m past the starting line) until the initiation of shoulder rotation, or until the participant passed through the door if no shoulder rotation occurred. Following the practices of Muroi & Higuchi (2017), we considered shoulder rotation onset to occur when the angle

of shoulder rotation deviated by more than 4 standard deviations from the average shoulder rotation angle in the initial 1.5 meters of sustained walking (See Figure 13).

Table 7

List of Aperture Crossing Behavior Variables

Variable Name (units)	Description of variable
Collision (Y/N)	Experimenter observation. Occurrence of the bar colliding with the aperture on each trial (Y/N).
Location of collision (R/L)	Experimenter observation. Collision with the left or right column.
Shoulder rotation (Y/N)	Shoulder rotation occurs if the shoulder angle deviates by more than 4 standard deviations from the average shoulder angle of the initial 1.5 meters of sustained walking, OR if the shoulder angle at crossing exceeds 20 degrees.
Direction of rotation (R/L)	Indicated by whether the Left or Right tracker on the bar passes through the aperture first.
Midpoint of the bar at the time of crossing (cm)	X-position distance between the left column and the midpoint of the bar (cm) when the midpoint of the bar passes through the aperture. See Figure *14*.
Midpoint of body at the time of crossing (cm)	X-position distance between the left column and the midpoint of the shoulders (cm) when the midpoint of the shoulders passes through the aperture.
Angle of rotation at crossing (deg.)	Absolute value of deviation from the fronto-parallel plane when the midpoint of the shoulders passes through the aperture.

The shoulder rotation at the time of crossing was determined by the shoulder angle (deviation from the fronto-parallel plane) when the midpoint of the bar passed through the aperture. The midpoint of the participant at the time of crossing was

determined by the average lateral position of the two trackers affixed to the participant's shoulders. Since the trackers affixed to the bar did not correspond to the midpoint of the bar for all bar configurations, the midpoint of the bar was computed by taking the lateral position of one bar tracker and adding a known displacement value based on the bar configuration. For example, if the bar extends 70 cm to the left of the tracker and 30 cm to the right of the tracker, then the midpoint of the bar can be calculated as 20 cm to the left of the location of the tracker. In order to account for instances where participants have rotated their shoulders (and the bar) while passing through the aperture, the location of the bar tracker will be combined with the cosine of the shoulder angle multiplied by the known displacement value, see Figure 14.

Figure 13

Experiment 2 Room Setup

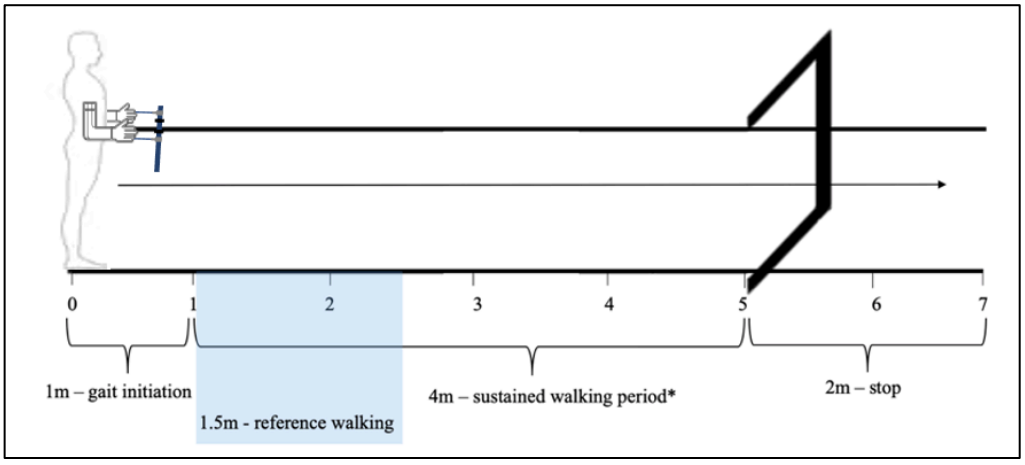

Figure 14

Calculation of Bar Midpoint for Unturned (left) and Turned (right) shoulders

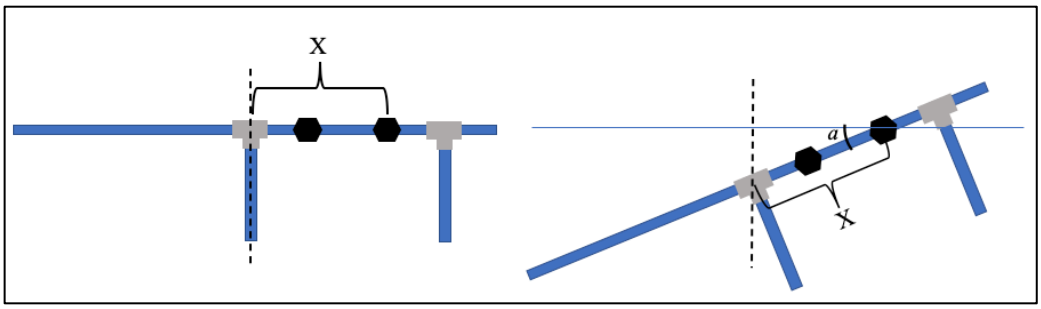

Note. Black dotted line represents the midpoint of the bar. X = a known displacement value between the right tracker and the midpoint of the bar. When the bar is not turned (left image), add X to the location of the tracker. When the bar is turned (right image), add the product of X and the cosine of the angle of the bar (a) to the location of the tracker.

Hierarchical Linear Modeling

Overview. For the same reasons as Experiment 1, hierarchical linear modeling (HLM) was used for analysis. Effect sizes and outlier analysis were conducted using the same techniques described in Experiment 1.

Binary Dependent Variables. The following dependent variables were dichotomous categorical variables: Collision (Y/N), Location of Collision (R/L), Shoulder Rotation (Y/N), and Direction of Rotation (R/L). Because these variables have only two possible outcomes, they produce a nonlinear cubic distribution. In order to utilize regression models such as HLM, the raw binary scores must be transformed into a linear distribution. This was completed using a binary logistic regression (Peng et al., 2002). The logistic regression model will predict the linear logit value, which can be later transformed into a probability score for interpretation.

To interpret the effects of continuous variables in a logistic regression, the regression coefficient (B) is converted into an odds ratio by taking the exponent of the coefficient (exp B). Instead of having an additive effect on the dependent variable, the odds ratio has a multiplicative effect (i.e., a one-unit increase in the predictor variable results in the odds being *multiplied* by the odds coefficient).

For a dichotomous dependent variable, the R^2 is calculated by taking the ratio of explained variance to total variance (Snijders & Bosker, 2012). Explained variance is calculated as the variance of the predicted logit values. Total variance is the sum of the predicted logit variance, the intercept variance (unexplained variance at Level 2), and the residual variance (unexplained variance at Level 1, denoted as a constant value of 3.29). Thus, the R^2 for binary HLM models will be calculated using the equation below:

$$R^2 = \frac{predicted\ logit\ variance}{predicted\ logit\ variance + intercept\ variance + 3.29}$$

Predicting Centering Behavior

Midpoint of the Body at Crossing. A hierarchical linear model was used to assess the effects of Trial, Aperture Width, and Bar Configuration on the midpoint of the body at the time of aperture crossing. As a reminder, a positional value of zero represents the left frame of the aperture, and positional values that increase indicate the midpoint of the body moving to the right. See Table 8 for results of the model. Holding all variables at their average (aperture width = 115cm, bar configuration = 50L/50R), participants' body midpoints were 59.96 cm away from the left post of the aperture at the time of crossing. Thus, on average the participants walked through the aperture so that their

bodies were at a location very close to its center (i.e., the midpoint of a 115 cm aperture is 57.5 cm).

A main effect of trial revealed that the midpoint of the body moved slightly to the left (B = -.04) over time, regardless of aperture width and bar configuration. As expected there was a significant main effect of aperture width, such that as the aperture width increases by 1 cm, the midpoint of the participant's body moved .96 cm further away from the left post of the aperture. This effect accounted for 75% of the residual variance in the model, and the slope coefficient for the effect of aperture width was larger than anticipated. For reference, if the body midpoint were to remain in the center of the aperture, we would expect to see a 0.5 cm change in position for every 1cm increase in aperture width. Results suggest that participants were almost doubling the magnitude of the expected effect. Similarly, the participant's shoulder angle when passing through the aperture was a strong predictor, accounting for 11% of the residual variance. For each additional degree of shoulder rotation, the midpoint of the body moved further to the right by 0.25 cm.

Further, there was a significant main effect of the bar configuration, accounting for 4% of the intercept variance. As the bar configuration changed incrementally from 70L/30R to 60L/40R to 50L/50R and so on, the intercept of the regression equation shifted 3.18 cm leftward. This indicates that as the center of the object was positioned more to the right of the body midline, participants compensated by walking more to the left. This is depicted in Figure 15 by the line for each bar configuration being at a different height. However, this shift

Table 8

Regression Coefficients for Fixed Effects Predicting the Midpoint of the Body at Crossing in Experiment 2

Predictor	B	SE	df	t	sr^2
Intercept	59.96	1.78	27	33.6***	--
Trial	-0.046	0.009	1971	-4.75***	0.001
Aperture Width	0.96	0.01	1971	94.55***	0.75
Shoulder Angle	0.25	0.006	1976	36.46***	0.11
Bar Configuration	-3.18	0.15	1980	-21.22***	0.04
Driving Experience	-0.85	2.07	25	-0.41	--
Trial * Aperture Width	.00008	.0004	1970	0.18	--
Trial * Bar configuration	-0.007	0.007	1981	-0.9	--
Aperture Width * Bar Configuration	-0.014	0.007	1967	-1.93	--
Trial * Aperture Width * Bar Config	0.0002	0.0003	1959	0.73	--

Figure 15

Midpoint of the Body at Crossing by Aperture Width and Bar Configuration

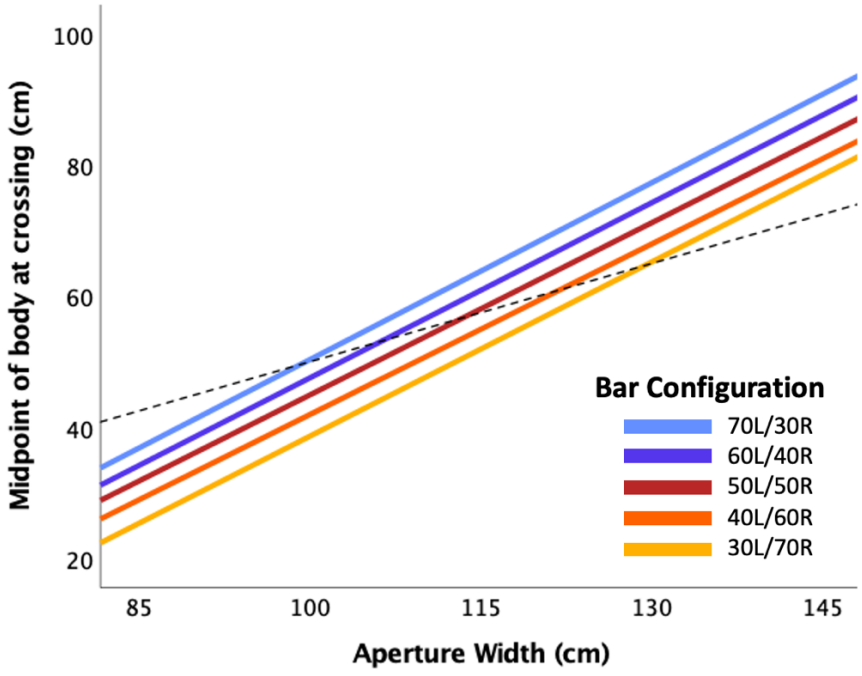

Note. The dotted line represents the true center of each aperture width.

was on average only 3.18 cm, which is much less than the 10 cm shift of the body that would have been required to center the person-plus-object system.

Midpoint of the Bar at crossing. A hierarchical linear model was used to assess the effects of Trial, Aperture Width, Bar Configuration, and shoulder rotation on the midpoint of the bar at the time of aperture crossing. Because categorical predictors were included in this model, both the omnibus F results and the regression coefficients are presented. See Table 9 for results of the omnibus F test and Table 10 for regression coefficients.

Table 9

Omnibus F Test Results for Fixed Effects Predicting the Midpoint of the Bar at Crossing in Experiment 2

Predictor	F	df1	df2	sig	sr^2
Trial	28.7	1	1961	<0.001	0.004
Aperture Width	3808.9	1	1963	<0.001	0.55
Shoulder Angle	558.2	1	1985	<0.001	0.01
Direction of Rotation	692.6	1	1987	<0.001	0.09
Bar Configuration	196.8	1	1962	<0.001	0.02
Trial * Aperture Width	0.29	1	1960	0.59	--
Shoulder Angle * Direction of Rotation	1901.8	1	1974	<0.001	0.14
Trial * Bar Configuration	3.24	1	1981	0.07	--
Aperture Width * Bar Configuration	0.02	1	1960	0.8	--
Shoulder Angle * Bar Configuration	368.0	1	1961	<0.001	0.044
Direction of Rotation * Bar Configuration	22.1	1	1972	<0.001	0.002
Trial * Aperture Width * Bar Configuration	1.9	1	1958	0.17	--

Table 10

Regression Coefficients for Fixed Effects Predicting the Midpoint of the Bar at Crossing in Experiment 2

Predictor	B	SE	df	t
Intercept	48.62	2.09	34.3	23.26***
Trial	-0.08	0.01	1962	-5.84***
Aperture Width	0.94	0.02	1962	61.7***
Shoulder Angle	0.24	0.01	1972	23.6***
Bar Configuration	3.17	0.22	1963	14.03***
Trial * Aperture Width	-.0004	.0007	1960	-0.54
Trial * Bar Configuration	0.02	0.01	1981	1.79
Aperture Width * Bar Configuration	0.002	0.01	1960	0.13
Shoulder Angle * Bar Configuration	0.12	0.006	1961	19.9***
Trial * Aperture Width * Bar Configuration	0.0006	0.0005	1958	1.3

Note. *** denotes $p < .001$, ** denotes $p < .01$, * denotes $p < .05$

The average position of the midpoint of the bar across all phases and conditions was 48.6 cm away from the left post of the aperture. In other words, when holding the bar configuration at 50L/50R and the aperture width at 115 cm, the midpoint of the bar was about 10 cm to the left of the true midpoint of the aperture (57.5 cm). There was a main effect of trial resulting in the midpoint of the bar moving slightly further to the left (B = -0.08) over time. Again, a main effect of the aperture width revealed that as the aperture width increased by 1cm, the midpoint of the bar moved 0.94 cm to the right. The size of this slope coefficient was expected to be less steep (closer to 0.5), such that as the aperture width increased, the midpoint of the bar remained in the center of the aperture. This can be seen in Figure 16 by comparing the slopes each bar configuration with the slope of the dotted black line representing the midpoint of the aperture. Further, a main effect of bar configuration revealed that as the configuration changed incrementally from

70L/30R to 30L/70R, the midpoint of the bar moved 3.17 cm to the right. As depicted in Figure 16, this suggests that when the bar extended further to the right, participants moved through the aperture so that the midpoint of the bar was closer to the right post of the aperture.

The shoulder angle at crossing and the direction of rotation were both significant predictors of the midpoint of the bar, together accounting for over 10% of the residual variance. As the angle of shoulder rotation at crossing increased by 1 degree, the midpoint of the bar moved 0.24 cm further to the right. This effect is further qualified by a main effect of the direction of rotation. When participants rotated so that the right side of the bar passed through the aperture first (i.e., they turned so that their back was towards the right post of the aperture), the average midpoint of the bar was significantly further to the left (M = 43.52, SE = 1.98) compared to when participants rotated so that the left side of the bar went through the aperture first (M = 64.21, SE = 1.95, $t(1987)$ = 27.07, $p < 0.001$). In other words, when the participant turned their back to the left post of the aperture, the bar was displaced further from that side of the aperture (i.e., the participant's body and forearm length were put in between the left post of the aperture and the midpoint of the bar itself).

Further, the effect of shoulder rotation was significantly moderated by the direction of rotation. A post-hoc test of simple slopes revealed that when participants rotated so that the right side of the bar passed through the aperture first, the effect of shoulder angle was a negative slope (B = -0.31, SE = 0.02), and when participants rotated so that the left side of the bar passed through the aperture first, the effect of shoulder

angle was a positive slope (B = 0.36, SE = 0.01, t(1974) = -44.4, p < 0.001). This can also be explained by the fact that the direction of rotation itself makes the midpoint of the bar further or closer to the fixed right side of the aperture.

Figure 16

Midpoint of the Bar at Crossing by Aperture Width and Bar Configuration

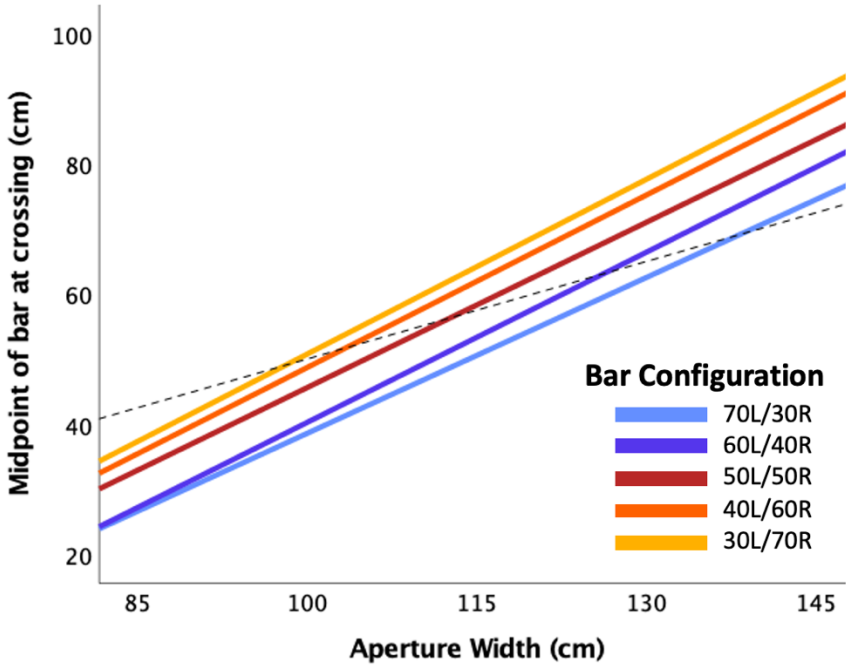

Note. The dotted line represents the true center of each aperture width.

Additionally, the bar configuration significantly moderated the effect of shoulder angle. A test of simple slopes revealed that the effect of shoulder angle on the midpoint of the bar was shallower for bar configurations that extended further to the left (70L/30R: B = -0.002, SE = 0.01, t (1961) = -0.1, p = .9) and steeper for bar configurations that extended further to the right (30L/70R: B = 0.48, SE = 0.01, t (1961) = 30.6, p <0.001),

see Figure 17. This is an artifact of using the left side of the aperture as the reference point; As the midpoint of the bar shifts further from the reference point on the left side of the aperture (i.e., the bar configuration extends further to the left), the rotation of the bar results in larger displacements of the lateral position of the midpoint.

Lastly, the direction of rotation significantly moderated the effect of bar configuration. When participants led with the right side of the bar, each incremental change in bar configuration from 70L/30R to 30L/70R resulted in a larger shift of the intercept to the right ($B = 4.53$, $SE = 0.35$, $t(1967) = 12.68$, $p < 0.001$) compared to when participants led with the left side of the bar ($B = 2.24$, $SE = 0.47$, $t\ (1967) = 4.69$, $p < 0.001$).

Figure 17

Midpoint of the Bar at Crossing by Shoulder Angle and Bar Configuration

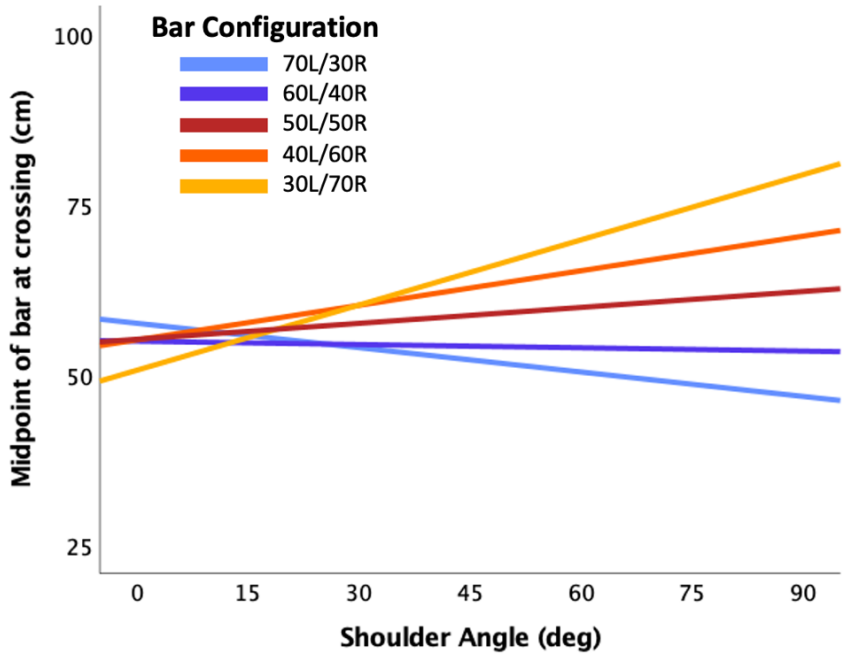

Due to the major influences of shoulder rotations on the midpoint of the bar at crossing, a supplemental analysis was conducted only on trials in which participants did not turn their shoulders to assess whether participants centered the midpoint of the bar when their shoulders remained parallel to the aperture. The data file was filtered so that only trials in which participants did not turn their shoulders were used. The resulting data included 558 trials, with an equal distribution of all five bar configurations and the largest three aperture widths (115, 130, and 145cm). See Table 11 for results of the model.

Table 11

Regression Coefficients Predicting the Midpoint of the Bar at Crossing for Trials when the Participant Did Not Turn Their Shoulders

Predictor	B	SE	df	t	sr^2
Intercept	67.59	1.91	30	35.31^{***}	--
Trial	-0.08	0.01	529	-6.36^{***}	0.02
Aperture Width	0.91	0.02	528	40.27^{***}	0.74
Bar Configuration	-0.58	0.19	528	-3.03^{**}	0.005
Trial*Aperture Width	0.002	0.001	527	1.66	--
Trial * Bar Configuration	-0.005	0.01	535	-0.46	--
Aperture Width * Bar Config	0.006	0.02	527	0.35	--
Trial * Aperture Width * Bar Config	0.002	0.002	526	-1.1	--

Note. *** denotes $p < .001$, ** denotes $p < .01$, * denotes $p < .05$

Holding this smaller dataset at its average aperture width (130 cm) and bar configuration (50L/50R), on average participants were successfully passing through the aperture such that the midpoint of the bar was at the center of the aperture (*intercept* = 67.59, midpoint of 130 cm = 65 cm). Similar to the full model, there was a main effect of trial (B = -0.08) and a main effect of aperture width (B = 0.91), such that the midpoint of

the bar moved further to the left as participants completed more trials and further to the right as the aperture width increased. As with the full model, the effect of aperture width was steeper than expected, since the slope coefficient would need to be closer to 0.5 in order for participants to find the true midpoint of the aperture. Lastly, there was a main effect of bar configuration that, although significant, was a smaller effect compared to when running the full model. For the full model (including trials in which participants rotated their shoulders), the midpoint of the bar moved leftward 3cm for each incremental change in bar configuration. As seen in Figure 18, when participants were not turning their shoulders, the midpoint of the bar only moved 0.58cm left for each incremental change in bar configuration. This suggests that when participants' shoulders remained parallel to the aperture, they behaved more similarly across all bar configurations.

Figure 18

Midpoint of the Bar at Crossing by Aperture Width and Bar Configuration for Trials when the Participant Did Not Turn their Shoulders

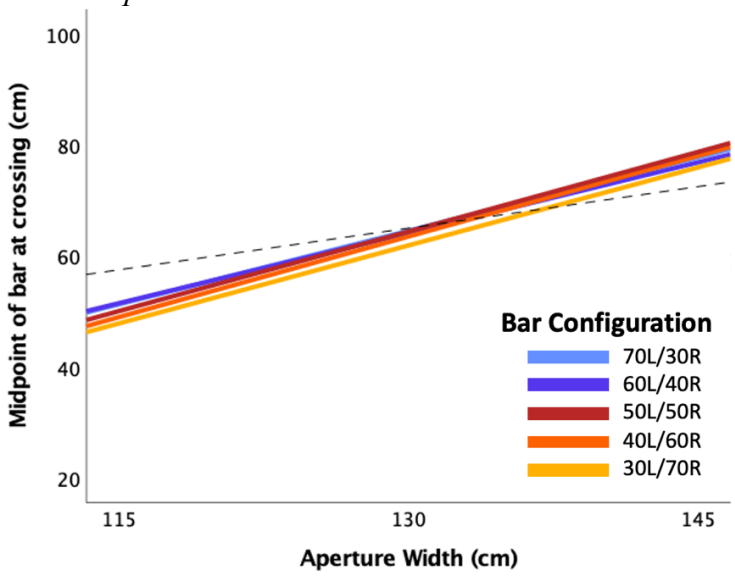

Note. The dotted line represents the true center of each aperture width.

Predicting Other Aperture Crossing Variables

Probability of Shoulder Rotation. A binary logistic hierarchical linear model was used to assess the effects of trial, aperture width, and bar configuration on the likelihood of participants rotating their shoulders, see Table 12.

Table 12

Regression Coefficients for Fixed Effects Predicting Shoulder Rotation

Predictor	B	SE	exp(B)	df	t	sr^2
Intercept	0.34	0.13	1.41	2091	2.68**	--
Trial	0.006	0.002	1.006	2091	2.99**	0.005
Aperture Width	-0.013	0.002	0.99	2091	-6.08***	0.022
Bar Configuration	0.07	0.03	1.08	2091	2.26*	0.003
Driving Experience	-0.04	0.11	0.96	20	-0.38	--
Trial * Aperture Width	-.0006	.0009	1	2090	-0.07	--
Trial * Bar Configuration	-0.002	0.001	0.998	2090	-1.38	--
Aperture Width * Bar Config	0.001	0.002	1.001	2090	0.36	--
Trial * Aperture Width * Bar Config	0	.006	1	2087	1.85	--

Note. *** denotes p < .001, ** denotes p < .01, * denotes p < .05

Holding all variables at their average, there was a .59 probability of a participant turning their shoulders on a given trial (recall that the logit values are presented in the results table, and must be converted into odds and probabilities for interpretation). A main effect of trial revealed that for each additional trial, the odds of rotating the shoulders increased slightly by a multiplicative factor of 1.006. Further, there was a significant main effect of aperture width, such that an increase in aperture width slightly decreased the odds of rotating the shoulders (*exp(B)* = 0.99). Lastly, there was a

significant main effect of the bar configuration. As the bar configuration incrementally changed from 70L/30R to 30L/70R, the odds of a participant rotating their shoulders increased by a multiplicative effect of 1.08. This suggests that participants were rotating their shoulders more often when the bar configuration extended further to the right. There were no significant interactions between trial, aperture width, or bar configuration.

Direction of Rotation. A binary logistic hierarchical linear model was used to assess the effects of trial, aperture width, and bar configuration on the direction of shoulder rotation (whether participants led with the left or right shoulder). For this model, only trials in which participants rotated their shoulders were included (N = 1222). The reference value for this analysis was a right rotation, so the following results are predicting the probability that the participant led with their right shoulder when turning through the aperture. See Table 13 for results of the model.

Table 13

Regression Coefficients for Fixed Effects Predicting Right Shoulder Rotations

Predictor	B	SE	exp(B)	df	t	sr^2
Intercept	-0.67	0.64	0.512	1216	1.05	--
Trial	0.007	0.003	1.01	1216	2.02*	0.002
Aperture Width	-0.003	0.004	0.997	1216	-0.69	--
Bar Configuration	-0.27	0.06	0.76	1216	-4.9***	0.008
Driving Experience	0.78	0.73	2.18	20	1.06	--
Trial * Aperture Width	-0.001	0.002	1	1215	-0.869	--
Trial * Bar Configuration	-0.006	0.003	0.99	1215	-1.27*	0.005
Aperture Width * Bar Config	-0.005	0.003	0.001	1215	-1.71	--
Trial * Aperture Width * Bar Config	0.0007	0.0001	1	1212	-0.58	--

Note. *** denotes $p < .001$, ** denotes $p < .01$, * denotes $p < .05$

Holding all variables at their average, there was a .34 probability that a participant led with their right shoulder. A main effect of trial revealed that for each additional trial, the odds of rotating the shoulders to the right increased slightly by a multiplicative factor of 1.01. There was also a main effect of bar configuration. As the bar configuration incrementally changed from 70L/30R to 30L/70R, participants were less likely to turn their shoulders to the right (*exp(B)* = 0.76). In other words, participants were more likely to rotate their shoulders so that the shorter end of the bar passed through the door first. Lastly, the main effect of trial was significantly moderated by the bar configuration. To assess the simple slopes, the file was split by bar configuration and the analysis was re-run. Simple slopes revealed that the main effect of trial was only significant for leftward extending bar configurations (30L/70R: $B = 0.14$, $SE = 0.03$, *exp(B)* = 1.15, $t\ (232) = 3.92$, $p < 0.001$), but was not different from zero for the symmetrical bar configuration (50R:50L: $B = 0.05$, $SE = 0.03$, *exp(B)* = 1.05, $t\ (225) = 1.5$, $p = 0.14$) or the rightward extending bar configurations (70L/30R: $B = -.002$, $SE = 0.03$, *exp(B)* = 0.99, $t\ (260) = -0.08$, $p = .93$). For the bar configurations that extended further to the left, the likelihood of turning the right side (e.g., the shorter side) of the bar through the aperture first increased as the participant completed more trials.

Shoulder Rotation Angle at Crossing. To further understand participants' aperture crossing behaviors, the angle of shoulder rotation at crossing was submitted to a hierarchical linear model. Higher angles represent a larger rotation of the shoulders, with a 90 degree rotation indicating that the participant was perpendicular to the aperture. See Table 14 for results of the model.

On average, participants' shoulders rotated to about 40 degrees. There was a main effect of trial such that participants rotated their shoulders slightly more as they completed more trials. There was also a main effect of aperture width. For every 1cm increase in aperture width, participants reduced their shoulder rotation by 0.2 degrees. The bar configuration did not significantly impact shoulder angle, nor did bar configuration significantly moderated any main effects.

Table 14

Regression Coefficients for Fixed Effects Predicting Shoulder Rotation Angle at Crossing

Predictor	B	SE	df	t	sr^2
Intercept	39.56	2.42	43.9	16.32***	--
Trial	0.07	0.03	2068	2.26*	0.002
Aperture Width	-0.211	0.03	2068	-6.59***	0.020
Bar Configuration	0.88	0.48	2068	1.84	--
Driving Experience	0.88	2.28	26	0.49	--
Trial * Aperture Width	0.001	0.001	2067	0.38	--
Trial * Bar Configuration	-0.03	0.02	2053	-1.24	--
Aperture Width * Bar Config	-0.009	0.02	2067	-0.39	--
Trial * Aperture Width * Bar Config	0.0010	0.0010	2064	1.28	--

Note. *** denotes $p < .001$, ** denotes $p < .01$, * denotes $p < .05$

Probability of Collision. Across all data, 97% of trials did not result in a collision with the aperture. Because there was not a sufficient number of trials in which collisions occurred to support a binary logistic regression, this variable will not be analyzed. The trials in which collisions occurred were scattered across multiple participants. Although there were not enough trials to conduct statistical analyses, frequency distributions suggest that almost half of all collisions occurred within the first

Figure 19

Frequency of Collisions by Trial

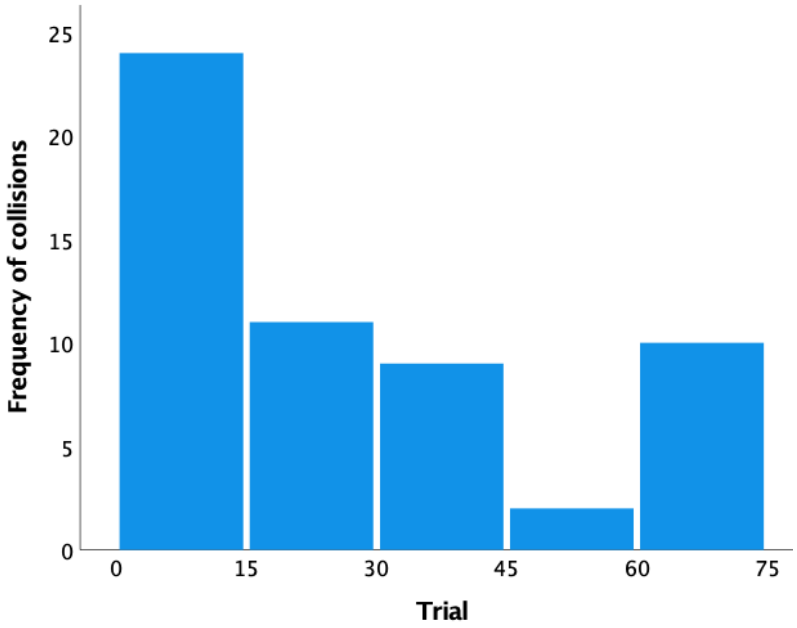

Figure 20

Frequency of Collisions by Bar Configuration

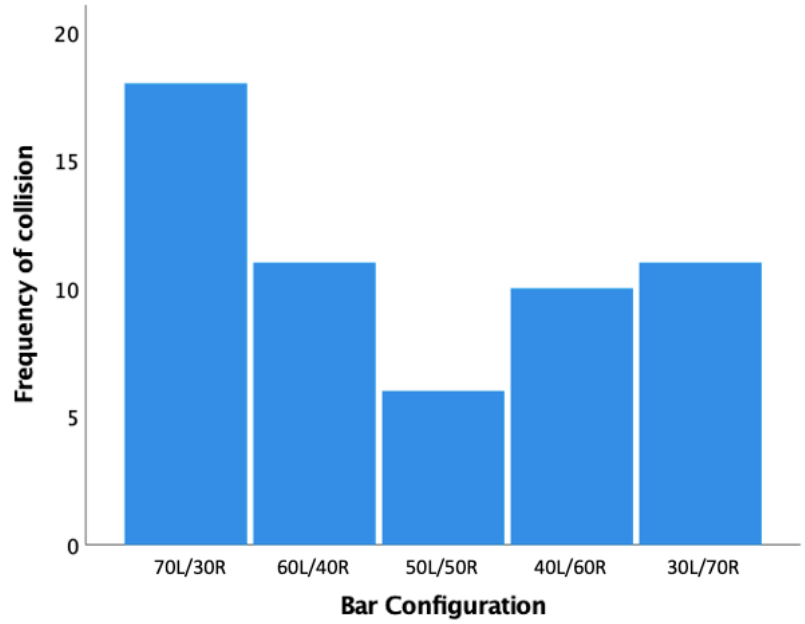

10 trials, and that collisions occurred more often for the asymmetrical bar configurations, see Figure 19 and Figure 20.

Location of Collision (L/R). As above, there were not enough trials that resulted in collisions to support a statistical analysis of the location of collision. However, frequency distributions suggest that participants typically collided with the side of the aperture corresponding to the side of the bar that extended further. Bar configurations extending further to the left resulted in collisions on the left side of the aperture, and bar configurations extending further to the right resulted in collisions on the right side of the aperture, see Figure 21.

Figure 21

Frequency of Left and Right Side Collisions by Bar Configuration

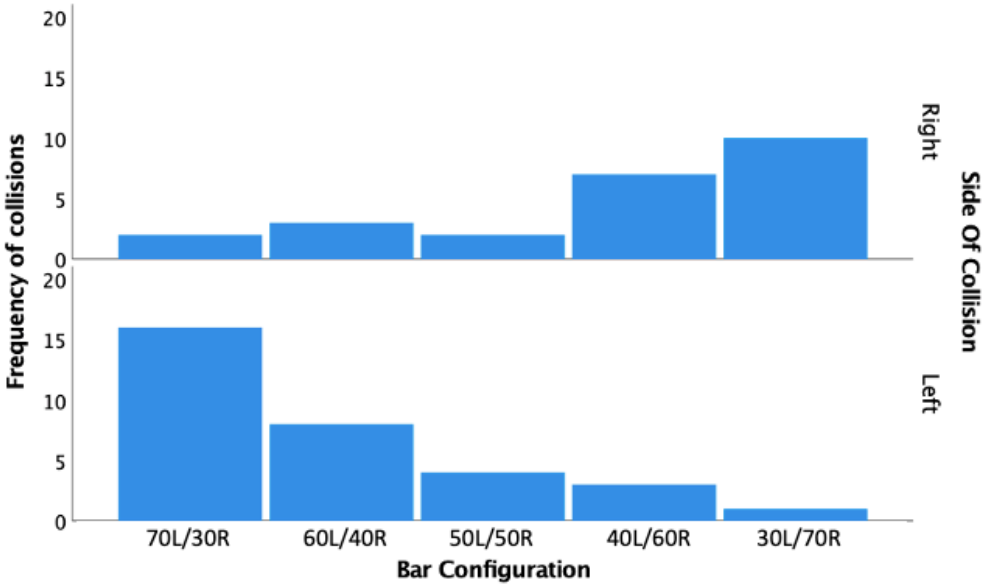

Discussion

The goal of Experiment 2 was to further understand how actors interact with their environment when a handheld tool generates an asymmetrical person-plus-object system. Participants walked through apertures of various widths while holding an asymmetrical bar, and motion tracking data from each trial were used to calculate a multitude of aperture crossing metrics. To assess whether participants moved through the aperture in ways predicted by the generalized control law (Equation 2), we analyzed the midpoint of the body and the midpoint of the bar at the time of crossing. We expected to see results that mimicked that of Experiment 1, such that participants centered the bar through the aperture, regardless of the bar configuration. Additional exploratory variables allowed us to assess changes in participants' safety buffer (shoulder rotation) and overall task success (collision) across bar configurations.

Body and Bar Positioning

When an actor engages in tool use, they functionally incorporate the properties of the tool such that the tool becomes an extension of the body (Berti & Frassinetti, 2000; Pagano & Turvey, 1998) and action capabilities are perceived in relation to this person-plus-object system (Day et al., 2017; Hackney et al., 2014; Wagman & Carello, 2003; Wagman & Taylor, 2005). In reference to the current study, we expected participants to pass through apertures such that they centered the overall person-plus-object system within the aperture, thereby maximizing the distance between the edges of the bar and the edges of the aperture and minimizing the likelihood of a collision. Since we manipulated the symmetry levels of the horizontal bar, we expected participants to laterally shift their

body so that the overall person-plus-object system (the bar) was always centered within the aperture, following the system asymmetry component of Equation 2.

In the symmetrical bar condition (50L/50R), participants positioned their bodies to be very close to the center of the aperture, replicating previous research on naturally symmetrical humans and animals (Higuchi et al., 2006). As the aperture width increased, the midpoint of the participants' body at the time of crossing shifted toward the new center of the aperture. Interestingly, participants moved about twice as far as they should have; Instead of shifting 0.5 cm for every 1 cm increase in aperture width, on average they shifted 0.96 cm. As a result, participants tended to pass through the aperture so that the midpoint of their body was to the left of the aperture midpoint for smaller aperture widths and to the right of the aperture midpoint for larger aperture widths (see Figure 15). Across all aperture widths for the symmetrical bar configuration, however, the average midpoint of the body never exceeded around 15 cm of error.

Importantly, participants shifted the position of their bodies at the moment of passing to account for the asymmetry of the horizontal bar. Participants consistently shifted their bodies away from the longer side of the asymmetrical bar, effectively moving the midpoint of the bar itself closer to the center of the aperture. Compared to Experiment 1, where participants shifted about 94% of the expected distance according to the generalized control law, participants in Experiment 2 only shifted around 30% of the expected distance. This could be an artifact of task instructions. In Experiment 1, participants were explicitly instructed to move to the center of the hallway. In Experiment 2, participants were instructed to pass through the aperture naturally, but they were not

outright asked to aim for the middle of the aperture. Perhaps the smaller shifts in body position were sufficient for participants to successfully pass through the aperture without contacting the sides of the doorway. The expected magnitude of body shifting may have also been attenuated by the shoulder rotations of the participant, which would have reduced the frontal width of the PPO and thus the necessary positional shifts for safe passage.

We expected to see the position of the midpoint of the bar converge at the midpoint of the aperture for all bar configurations, similar to the effects found in Experiment 1 (see Figure 8), as this would suggest that participants were accurately perceiving the asymmetry of the bar configuration and moving through the aperture in a way that placed the larger person-plus-object system at the center of the aperture. Instead, the midpoint of the bar when crossing through the aperture was systematically shifted according to the bar configuration, such that the 70L/30R bar midpoint was around 3cm to the left of the 60L/40R bar midpoint, and so on. This suggests that participants did not shift their bodies *far enough* to account for the full length of the asymmetrical bar. For every 10 cm shift in the bar's midpoint, participants shifted their bodies only 7 cm in the opposite direction.

However, the analyses revealed that the midpoint of the bar at the time of passing through the aperture was largely impacted by the direction and magnitude of shoulder rotation on any given trial. Because participants were holding the bar in front of their bodies, any rotation of the shoulders (the participants shoulders and the bar were fixed, so shoulder rotations resulted in a matching rotation of the bar) necessarily moved the

midpoint of the bar toward or away from the left post of the aperture, depending on the direction of rotation. If participants rotated their shoulders so that their back was turned to the left post of the aperture, the midpoint of the bar was shifted to the right, and vice versa. Further, the extent to which the midpoint of the bar shifted left or right depended on the magnitude of shoulder rotation. For example, a shoulder rotation of 90°, in which the participant's body and the bar were perpendicular to the aperture, resulted in the midpoint of the bar shifting an amount determined by the participant's elbow-to-hand length plus the length of the handles attached to the bar.

This highlights an important limitation of the metrics used in this experiment: as the participant rotates their shoulders, neither the midpoint of the bar not the midpoint of the participant's body accurately represent the midpoint of the person-plus-object system. Figure 22 shows an example of how shoulder rotation can result in the midpoint of the bar not equating to the midpoint of the PPO. As participants rotate their shoulders further, the midpoint of the bar extends further from the true midpoint of the PPO, and this effect is larger for asymmetrical systems compared to the symmetrical (50L/50R) system. Indeed, other researchers have suggested that if actors rotate their shoulders when crossing an aperture, placing the system in the exact center of the aperture may not be an important action parameter of task success (Higuchi et al., 2006). Future research could explore this further by including an additional metric: the midpoint of the overall person-plus-object system (denoted in Figure 22 as the dotted black line), which changes based on the length of participant's arms, the level of bar asymmetry, the direction of shoulder rotation, and the magnitude of shoulder rotation.

Figure 22

Effect of Shoulder Rotation on the Midpoint of the Bar

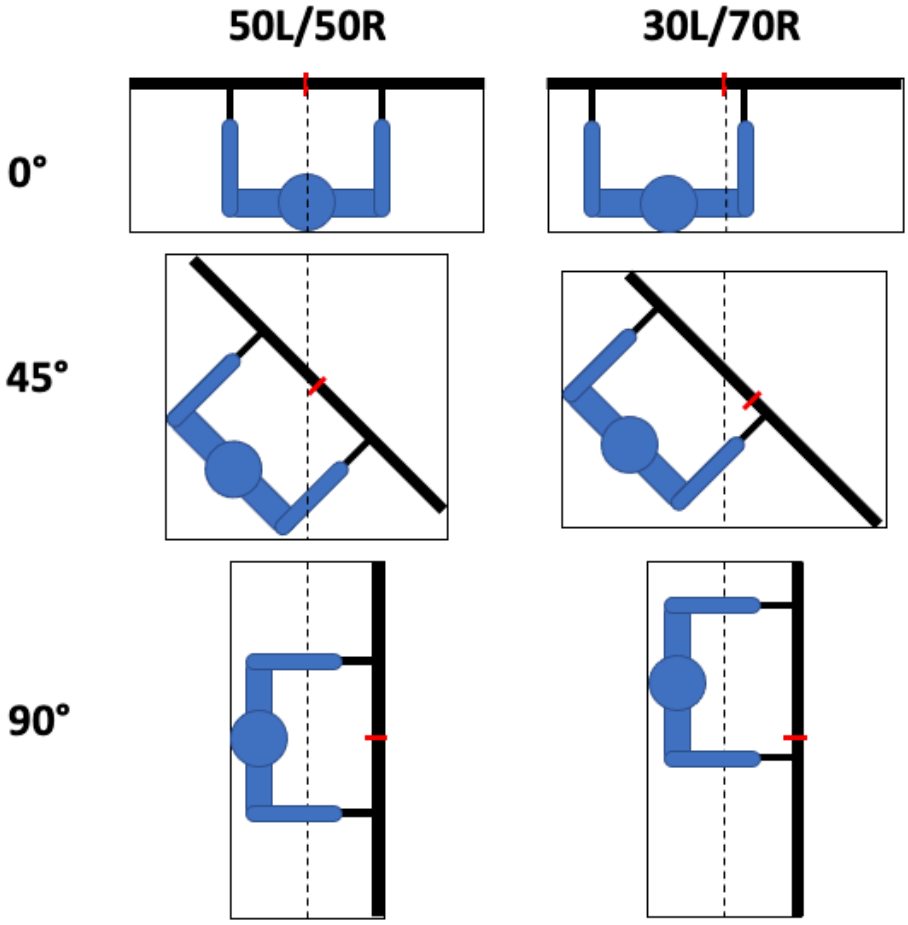

Note. The red hash represents the position of the midpoint of the bar, and the dotted black line represents the true midpoint of the person-plus-object system. As the actor rotates their shoulders, the midpoint of the bar shifts further away from the true midpoint of the person-pus-object system.

It is worth noting that some asymmetrical person-plus-object systems that people encounter in daily life, such as driving a vehicle, restrict the actor's ability to rotate the system during aperture passage. Future research should explore how aperture passing

behaviors change depending on the mode of transit (walking vs joystick/steering wheel) as well as whether or not the actor can rotate the system. A supplementary analysis studying only the trials in which participants did *not* rotate their shoulders was conducted to assess whether participants more accurately positioned the person-plus-object system in the center of the aperture while walking forward through the aperture. This restricted the analysis only to the larger aperture widths, but it ensured that the midpoint of the bar was an accurate metric for the midpoint of the PPO system. Promisingly, as seen in Figure 18, there was a close overlapping of the midpoint of the bar across all bar configurations. This replicates the results of Experiment 1 and suggests that when participants' shoulders remained parallel to the aperture, they more accurately shifted their bodies so that the center of the asymmetrical bar passed through the center of the aperture, regardless of the bar configuration.

Buffer Space (Shoulder Rotation)

In addition to centering the PPO system within the width of the aperture, rotating the overall system is another way to promote safe passage through an aperture. Since turning the shoulders reduces the frontal width of the actor, it can provide additional buffer space between the actor and the edges of the aperture (Franchak et al., 2012; Lucaites, Venkatakrishnan, Bhargava, et al., 2020; Warren & Whang, 1987; Wilmut & Barnett, 2010). Since participants were presented with aperture widths that were equal to (100 cm) or smaller than (85 cm) the width of the horizontal bar, we expected shoulder rotation to occur most for these aperture widths. Indeed, our results showed that participants were more likely to rotate their shoulders as the aperture width got smaller.

Participants were also more likely to rotate their shoulders when the bar configuration extended further to the right. This is an interesting finding, since each bar configuration had a total length of 100 cm. This suggests that whether or not an actor rotates their shoulders when passing through an aperture depends on more than just the ratio of frontal width to presented aperture width, and that actors may increase their buffers depending on the level of experience and practice they have had with a given scenario (Jones et al., 2011).

Previous research studying symmetrical PPO systems found that participants walking through apertures preferred to rotate their bodies in the same direction for every trial (Higuchi et al., 2012). Results of the present study, however, suggest that when presented with asymmetrical bar configurations, actors change their direction of rotation so that the shorter end of the bar passes through the aperture first.

When assessing the angle of rotation during aperture passing, a large angle of rotation indicates a larger buffer because it reduces the PPO system's frontal width and increases the likelihood of safe passage through the aperture. Replicating previous work, we found that the angle of shoulder rotation was proportional to the presented aperture width, such that smaller aperture widths required larger shoulder rotations (Higuchi et al., 2011; Lucaites, Venkatakrishnan, Bhargava, et al., 2020; Warren & Whang, 1987; Wilmut et al., 2015; Wilmut & Barnett, 2010). While the asymmetry of the bar increased participant's likelihood of rotating their shoulders at all, it did not significantly impact the angle of rotation. Thus, while the system asymmetry impacts whether or not an actor

engages in buffer-increasing behaviors such as shoulder rotations, the overall width of the system seems to be the major determinant of the magnitude of rotation.

Collisions

Overall, there were very few trials in which the bar collided with the aperture, a promising testament to our participants' ability to functionally incorporate the horizontal bar into their embodied action schema to promote safe movement throughout the environment (Day et al., 2017; Higuchi et al., 2006; Wagman & Taylor, 2005), even when the bar produced a novel asymmetrical system. Further, most collisions occurred toward the beginning of the experimental procedure, and the occurrence of collisions decreased as participants completed more trials. This trend replicates research suggesting that practicing a task allows for recalibration of the perception-action system (Bingham & Pagano, 1998; Day et al., 2017; Fajen, 2005; Franchak et al., 2010; Rieser et al., 1995), resulting in increased accuracy and precision within a perception-action task (E.J. Gibson & Pick, 2000).

Collisions occurred least often in the 50L/50R bar configuration and increased in occurrence as the degree of system asymmetry increased in either direction. This is likely an indication that participants were more experienced in walking through apertures with a symmetrical PPO system as opposed to an asymmetrical system. Further, when collisions did occur in the asymmetrical bar configurations, they most often occurred such that the longer side of the bar collided with the aperture. This could indicate that participants failed to adjust – or inaccurately adjusted – their lateral position considering

the asymmetry of the PPO system. A failure to laterally shift the body away from the long side of the bar would potentially result in a collision at the long side of the bar.

An eye tracking study by Kroll & Crundall (2019) found that drivers approaching an aperture looked longer and more often at the edge of the aperture closest to the driver's body (i.e., the edge closer to the shorter side of the asymmetrical person-plus-object system) because that side of the aperture had more behavioral urgency. In other words, because that side of the aperture is *closer* to the driver, it is more likely to cause personal harm than the aperture edge on the longer side of the PPO system, and is thus attended to more often (Franconeri & Simons, 2003). The finding that collisions occurred more often at the longer side of the asymmetrical PPO system, along with the trend that participants were more likely to rotate their shoulders so that the shorter end of the bar passed through the aperture first, aligns with this theory, suggesting that participants were more concerned with avoiding collision on the side closest to their bodies.

CHAPTER IV

General Discussion

Previous research has demonstrated that humans and animals steer down the center of a corridor by equalizing the speed of optic flow in the left and right fields of view (Bhagavatula et al., 2011; Duchon & Warren, 2002; Srinivasan, 1992; Srinivasan et al., 1991), a strategy in which optical information dynamically modulates perception-action processes without cognitively taxing motor commands (J. J. Gibson, 1979; Warren, 1998; Warren & Fajen, 2004). The optic flow equalization control law (Equation 1) assumes that the relevant perceptual organs (in this case, the eyes) are positioned symmetrically with respect to the rest of the body. If the actor's body is not bilaterally symmetrical to the point of observation, then optic flow equalization would not successfully center the body. While asymmetrical morphologies are rarely found in nature, humans engaging in tool use are often producing person-plus-object systems that are not laterally symmetrical.

Equation 2 presents a generalized optic flow equalization control law which specifies how centered steering of an asymmetrical system can be controlled through available perceptual information. First, the actor moves in such a way as to equalize the optic flow on the left and right fields of view (centering the eyes within the environment); Then, using visual and haptic information about the size and asymmetry of the person-plus-object system, the actor shifts the position of their eyes so that the true midpoint of the overall system replaces the position of the centered eyes. In Experiment 1, the efficacy of this generalized control law was tested by separately manipulating the

perceptual information for each part of the equation. Optic flow was manipulated by changing the speeds of two walls in a virtual hallway, and system asymmetry was manipulated by asking participants to hold a horizontal bar with varying degrees of asymmetry. Results showed that participants utilized information from both optic flow and system asymmetry to center themselves within the hallway, behaving as predicted by a weighted version of the generalized control law (see Equation 3).

In Experiment 2, participants held the asymmetrical bar as they walked through apertures of various widths. This experiment offered an opportunity to understand how an asymmetrical person-plus-object system would impact perception-action coordination for a more natural task. Participants were expected to utilize optic flow equalization strategies to center themselves within the aperture, accounting for the lateral asymmetry of their person-plus-object system. Results showed that participants accurately shifted the position of their bodies so that the overall person-plus-object system was centered through the aperture, but these results were complicated by rotations of the body when passing through the aperture. Overall, the present experiments provide evidence to suggest that the generalized control law (Equation 2) is used to support environmental navigation for multiple tasks in both real and virtual environments.

Contributions

Bilateral asymmetry presents a unique perception-action coordination problem because 1) it violates an assumption underlying every control law that relies on the equalization of a perceptual variable, optical or otherwise, and 2) it occurs frequently in daily life through PPO systems generated by handheld objects, vehicles, etc. For these

reasons, we believe that the present studies provide meaningful contributions to the science of visually-guided action. The results of the current studies demonstrate that humans engaging with an asymmetrical tool can 1) perceive the asymmetry of a person-plus-object system (both the full length of the tool and the segmented length of the tool extending to the left and right of the eyes), 2) use that information to modulate the use of optic flow equalization control laws for centered steering, and 3) functionally incorporate the asymmetrical tool into their perception-action system to successfully navigate their environment.

To our knowledge, this is the first empirical research to test the optic flow equalization control law for centered steering when tool use generates an asymmetrical person-plus-object system. Across both experiments, we found that participants could accurately perceive the midpoint of the bar (regardless of the bar configuration) and position their body so that the overall person-plus-object system was centered. These results occurred above and beyond any positional changes due to equalization of the optic flow. Overall, this provides evidence to support the use of the generalized control law (Equation 2) during steering tasks. This is an important discovery because it suggests that actors can dynamically adjust their action strategies to account for uniquely altered body states, and that control laws can be modified to utilize additional relevant perceptual information (in this case, visual and haptic information about the length and symmetry of the bar).

Wielding objects can change the actor-environment relationship by enhancing certain affordances and restricting others. In the case of objects that extend the frontal

width of the actor, opportunities for passing through apertures will be constrained by the total frontal width of the object. While previous research has demonstrated that humans are sensitive to affordances for aperture passability of the person-plus-object system (Higuchi et al., 2006; Lucaites, 2018; Wagman & Taylor, 2005), the current research further affirms that action strategies for passing through apertures is specific to the frontal width *and* the level of asymmetry of the person-plus-object system. Because participants passed through the aperture such that the asymmetrical bar was centered, we have further evidence that humans can perceive and utilize the information specified in the generalized control law.

Overall success in the aperture passability task suggests that participants were treating the horizontal bar as an extension of the body, and were perceiving and acting upon affordances for the integrated system. Participants successfully perceived the environmental layout in relation to the embodied action schema (Berti & Frassinetti, 2000; Day et al., 2017; Hirose & Nishio, 2001) produced by the horizontal bar. The manipulation of system asymmetry provides further support, and extends new context to embodied action schema research.

Future Research

The present studies are an initial attempt at answering the question of how actors perceive and act within an environment when tool use produces an asymmetrical system. Many additional questions emerged throughout the process of conducting and analyzing these experiments, and each experiment could become the basis of a larger research program. Below are possible avenues to extend the findings of each Experiment.

Extending Basic Research on Optic Flow Equalization (Experiment 1)

One of the unexpected findings from Experiment 1 was that participants only utilized optic flow equalization to travel 30% of the distance specified by the control law. A number of possible explanations were highlighted in the Experiment 1 Discussion, and offer a starting point for future research. First, as demonstrated in Figure 11, rotations of the body, head, and eyes likely impacts the extent to which optic flow information is available for perception. Future research should empirically evaluate the effects of head rotations on the use of optic flow equalization techniques, perhaps by measuring the amount of lateral adjustment that occurs when the head is or is not facing forward. It is possible that participants learn to sample the optic array for information specific to centering when they are facing forward with the focus of expansion at the center of the hallway or aperture, when the information is most accurate. Similarly, two hypotheses exist for which part of the optic flow field is being sampled during optic flow equalization: portions of the optic array that are perpendicular to the direction of gaze (Duchon & Warren, 2002), or portions of the optic array that are perpendicular to the direction of travel/heading (Srinivasan et al., 1991). Future research could test these hypotheses by experimentally manipulating which portions of the optic array are available for perception, and measuring the extent to which participants behave as predicated by the optic flow equalization control law.

Further, this basic research could be extended and improved by studying more naturalistic movements. While participants in the present experiment stepped left and right as self-motion was passively imposed by moving walls in the hallway, a better task

would allow participants to produce their own optic flow by asking them to walk down a hallway, further enhancing the level of perception-action coupling. Future work could also utilize a more naturalistic environment, which would include splay angles (implicit floors) and more realistic textures.

It is also worth noting that the generalized control law tested in the present experiment focused only on lateral components of optic flow, and assumed that the actors' goal was to center themselves laterally, but not vertically, within the environment. In most cases of human walking, actors navigate their environment by moving forward/backward and left/right, with relatively minimal vertical (up/down) movement. However, there are instances when a human would need to center their person-plus-object system both laterally and vertically, such as when flying an airplane or tele-operating a drone. Importantly, these examples represent instances when the human viewpoint may not be symmetrical to the vertical axis of the overall system (i.e., airplane pilots are not centered vertically within the plane; drone cameras are often placed above the vertical midpoint). Future work should assess the extent to which the optic flow equalization control law can be applied to lateral *and* vertical centering, especially for person-plus-object systems with varying levels of vertical and lateral asymmetry.

Applying Optic Flow Equalization to Realistic Passability Scenarios (Experiment 2)

There are a number of ways in which the asymmetrical person-plus-object system and experimental task can be adjusted to more closely mimic real-life scenarios, and each serves as an opportunity for future research. First, the current experiment utilized a horizontal bar to generate a person-plus-object system in which the bar always extended

beyond the shoulder width of the actor. Another scenario worth investigating is when the tool extends in one direction but not the other, such as when an actor holds a satchel or child that rests on one hip. In this case, actors would need to consider the extent to which their own body extends to one side, and the extent to which the tool or object extends to the other side, providing further evidence to the idea of an embodied action schema.

Further, this experiment utilized a walking task in which participants walked through various apertures, but an obvious opportunity for future research would utilize a different locomotion interface, such as steering via a joystick or steering wheel. These locomotion interfaces more closely resemble tasks such as driving an asymmetrical vehicle, tractor, or motorbike with side attachment. In the same vein, the task of driving a vehicle often eliminates the possibility of rotating the system, and future research should study how restricting rotations alters aperture passing behavior. In this case, other metrics of buffer space such as system speed can be utilized. Additionally, the current experiment offered both visual and haptic information about the length of the bar, but other realistic asymmetrical systems may offer only one informational source, or offer partial information. For example, vehicle drivers often do not receive haptic information about the width of the vehicle, and the visual information about the width of the vehicle can differ in its availability depending on its make and model. Research on the importance of line-of-sight visual information (Moore et al., 2009) about system asymmetry could provide meaningful insights into vehicle design and training.

Lastly, the bar configurations used to manipulate system asymmetry in the current experiment resulted in successful passability performance with very little collisions.

However, there was evidence within the collision data that calibration may have been occurring, because the prevalence of collisions lowered as participants completed more trials. For more challenging configurations of asymmetrical systems (e.g., tractors whose arm extensions can reach out as far as 20 feet in one direction), conducting research on calibration rates could provide meaningful insights for training best practices. Additional research should also recruit a more diverse set of participants – the undergraduate students in the current study had little variance in driving experience, but a future study may reveal a significant main effect of driving experience on the ability to navigate one's environment with an asymmetrical person-plus-object system.

Conclusion

The results of these experiments suggest that humans are sensitive to uniquely altered person-plus-object systems caused by asymmetrical tool use. Furthermore, humans attune to information about the symmetry of the person-plus-object system when perceiving affordances for passing through apertures and steering down hallways. These experiments provide evidence that perception-action systems can modulate their use of visual control laws depending on the properties of the system's morphology (size, shape, and symmetry), highlighting the emergent nature of complex and dynamic behavioral systems (Guastello et al., 2009; Riley & Van Orden, 2005).

References

Armbrüster, C., Wolter, M., Kuhlen, T., Spijkers, W., & Fimm, B. (2008). Depth perception in virtual reality: Distance estimations in peri- and extrapersonal space. *CyberPsychology & Behavior*, *11*(1), 9–15. https://doi.org/10.1089/cpb.2007.9935

Berti, A., & Frassinetti, F. (2000). When far becomes near: Remapping of space by tool use. *Journal of Cognitive Neuroscience*, *12*(3), 415–420. https://doi.org/10.1162/089892900562237

Bhagavatula, P. S., Claudianos, C., Ibbotson, M. R., & Srinivasan, M. V. (2011). Optic flow cues guide flight in birds. *Current Biology*, *21*(21), 1794–1799. https://doi.org/10.1016/j.cub.2011.09.009

Bhargava, A. (2020). The effect of anthropometric properties of self-avatars on action capabilities in virtual reality. *All Dissertations*, 137.

Bickel, R. (2007). *Multilevel analysis for applied regression: It's just regression!* Guilford Press.

Bingham, G. P., & Pagano, C. C. (1998). The necessity of a perception-action approach to definite distance perception: Monocular distance perception to guide reaching. *Journal of Experimental Psychology: Applied*, *24*(1), 24.

Burton, G., & Turvey, M. T. (1990). Perceiving the lengths of rods that are held but not wielded. *Ecological Psychology*, *2*(4), 295–324.

Burton, G., Turvey, M. T., & Solomon, H. Y. (1990). Can shape be perceived by dynamic touch? *Perception & Psychophysics*, *48*(5), 477–487. https://doi.org/10.3758/BF03211592

Chou, Y. H., Wagenaar, R. C., Saltzman, E., Giphart, J. E., Young, D., Davidsdottir, R., & Cronin-Golomb, A. (2009). Effects of optic flow speed and lateral flow asymmetry on locomotion in younger and older adults: A virtual reality study. *The Journals of Gerontology Series B: Psychological Sciences and Social Sciences*, *64B*(2), 222–231. https://doi.org/10.1093/geronb/gbp003

Cinelli, M. E., Patla, A. E., & Allard, F. (2009). Behaviour and gaze analyses during a goal-directed locomotor task. *The Quarterly Journal of Experimental Psychology*, *62*(3), 483–499. https://doi.org/10.1080/17470210802168583

Cohen, J., Cohen, P, West, S, & Aiken, L. (2003). *Applied multiple regression* (3rd ed.). Earlbaum.

Collett, T. S., & Land, M. F. (1975). Visual control of flight behaviour in the hoverflySyritta pipiens L. *Journal of Comparative Physiology ? A*, *99*(1), 1–66. https://doi.org/10.1007/BF01464710

Day, B., Ebrahimi, E., Hartman, L. S., Pagano, C. C., & Babu, S. V. (2017). Calibration to tool use during visually-guided reaching. *Acta Psychologica*, *181*, 27–39. https://doi.org/10.1016/j.actpsy.2017.09.014

Duchon, A. P., Kaelbling, L. P., & Warren, W. H. (1998). Ecological robotics. *Adaptive Behavior*, *6*(3–4), 473–507. https://doi.org/10.1177/105971239800600306

Duchon, A. P., & Warren, W. H. (2002). A visual equalization strategy for locomotor control: Of honeybees, robots, and humans. *Psychological Science*, *13*(3), 272–278. https://doi.org/10.1111/1467-9280.00450

Duchon, A. P., & Warren, W. H. (1994). Robot navigation from a Gibsonian viewpoint. *Proceedings of IEEE International Conference on Systems, Man and Cybernetics*, *3*, 2272–2277. https://doi.org/10.1109/ICSMC.1994.400203

Durgin, F. H., Pelah, A., Fox, L. F., Lewis, J., Kane, R., & Walley, K. A. (2005). Self-motion perception during locomotor recalibration: More than meets the eye. *Journal of Experimental Psychology: Human Perception and Performance*, *31*(3), 398–419. https://doi.org/10.1037/0096-1523.31.3.398

Fajen, B. R. (2005). Calibration, information, and control strategies for braking to avoid a collision. *Journal of Experimental Psychology: Human Perception and Performance*, *31*(3), 480–501. https://doi.org/10.1037/0096-1523.31.3.480

Fajen, B. R. (2007). Affordance-based control of visually guided action. *Ecological Psychology*, *19*(4), 383–410. https://doi.org/10.1080/10407410701557877

Franchak, J. M., Celano, E. C., & Adolph, K. E. (2012). Perception of passage through openings depends on the size of the body in motion. *Experimental Brain Research*, *223*(2), 301–310. https://doi.org/10.1007/s00221-012-3261-y

Franchak, J. M., van der Zalm, D. J., & Adolph, K. E. (2010). Learning by doing: Action performance facilitates affordance perception. *Vision Research*, *50*(24), 2758–2765. https://doi.org/10.1016/j.visres.2010.09.019

Franconeri, S. L., & Simons, D. J. (2003). Moving and looming stimuli capture attention. *Perception & Psychophysics*, *65*(7), 999–1010. https://doi.org/10.3758/BF03194829

Geuss, M. N., Stefanucci, J. K., Creem-Regehr, S. H., & Thompson, W. B. (2012). Effect of viewing plane on perceived distances in real and virtual environments. *Journal of Experimental Psychology: Human Perception and Performance*, *38*(5), 1242–1253. https://doi.org/10.1037/a0027524

Gibson, E. J., Gibson, J. J., Smith, O. W., & Flock, H. (1959). Motion parallax as a determinant of perceived depth. *Journal of Experimental Psychology*, *58*(1), 40–51. https://doi.org/10.1037/h0043883

Gibson, E.J., & Pick, A. D. (2000). *An ecological approach to perceptual learning and development*. Oxford University Press.

Gibson, J. J. (1950). *The Perception of the visual world*. Houghton Mifflin Company.

Gibson, J. J. (1958). Visually controlled locomotion and visual orientation in animals. *British Journal of Psychology*, *49*(3), 182–194. https://doi.org/10.1111/j.2044-8295.1958.tb00656.x

Gibson, J. J. (1961). Ecological optics. *Vision Research*, *1*, 253–262.

Gibson, J. J. (1966). *The senses considered as perceptual systems*. Houghton Mifflin Company.

Gibson, J. J. (1979). *The ecological approach to visual perception*. Houghton Mifflin.

Gibson, J. J., & Crooks, L. E. (1938). A theoretical field-analysis of automobile-driving. *The American Journal of Psychology*, *51*(3), 20.

Guastello, S., Koopmans, M., & Pincus, D. (2009). *Chaos and complexity in psychology: The theory of nonlinear dynamical systems*. Cambridge University Press.

Hackney, A. L., & Cinelli, M. E. (2013). Young and older adults use body-scaled information during a non-confined aperture crossing task. *Experimental Brain Research*, *225*(3), 419–429. https://doi.org/10.1007/s00221-012-3382-3

Hackney, A. L., Cinelli, M. E., & Frank, J. S. (2014). Is the critical point for aperture crossing adapted to the person-plus-object system? *Journal of Motor Behavior*, *46*(5), 319–327. https://doi.org/10.1080/00222895.2014.913002

Hajnal, A., Fonseca, S., Harrison, S., Kinsella-Shaw, J., & Carello, C. (2007). Comparison of dynamic (effortful) touch by hand and foot. *Journal of Motor Behavior*, *39*(2), 82–88. https://doi.org/10.3200/JMBR.39.2.82-88

Hartman, L. (2018). Perception-action system calibration in the presence of stable and unstable perceptual perturbations. *All Dissertations, Clemson University.* https://tigerprints.clemson.edu/all_dissertations/2144

Helmholtz, H. V. (1925). *Physiological optics (Vol. 3)*. Optical Society of America.

Higuchi, T., Chiba, M., & Kusumi, M. (2015). *Locomotion through apertures as the person-plus-object system: When the body is off the center*. 18th International Conference on Perception and Action, Minneapoils, MN.

Higuchi, T., Cinelli, M. E., Greig, M. A., & Patla, A. E. (2006). Locomotion through apertures when wider space for locomotion is necessary: Adaptation to artificially altered bodily states. *Experimental Brain Research*, *175*(1), 50–59. https://doi.org/10.1007/s00221-006-0525-4

Higuchi, T., Cinelli, M. E., & Patla, A. E. (2009). Gaze behavior during locomotion through apertures: The effect of locomotion forms. *Human Movement Science*, *28*(6), 760–771. https://doi.org/10.1016/j.humov.2009.07.012

Higuchi, T., Murai, G., Kijima, A., Seya, Y., Wagman, J. B., & Imanaka, K. (2011). Athletic experience influences shoulder rotations when running through apertures. *Human Movement Science*, *30*(3), 534–549. https://doi.org/10.1016/j.humov.2010.08.003

Higuchi, T., Seya, Y., & Imanaka, K. (2012). Rule for scaling shoulder rotation angles while walking through apertures. *PloS One*, *7*(10), e48123.

Higuchi, T., Takada, H., Matsuura, Y., & Imanaka, K. (2004). Visual estimation of spatial requirements for locomotion in novice wheelchair users. *Journal of Experimental Psychology: Applied*, *10*(1), 55–66. https://doi.org/10.1037/1076-898X.10.1.55

Hirose, N., & Nishio, A. (2001). The process of adaptation to perceiving new action capabilities. *Ecological Psychology*, *13*(1), 49–69. https://doi.org/10.1207/S15326969ECO1301_3

Hofmann, D. A. (1997). An overview of the logic and rationale of hierarchical linear models. *Journal of Management*, *23*(6), 723–744. https://doi.org/10.1177/014920639702300602

Holló, G., & Novák, M. (2012). The manoeuvrability hypothesis to explain the maintenance of bilateral symmetry in animal evolution. *Biology Direct*, *7*(1), 22. https://doi.org/10.1186/1745-6150-7-22

Jones, K. S., Johnson, B. R., & Schmidlin, E. A. (2011). Teleoperation through apertures: passability versus driveability. *Journal of Cognitive Engineering and Decision Making*, *5*(1), 10–28. https://doi.org/10.1177/1555343411399074

Knoll, A. H., & Carrol, S. B. (1999). Early animal evolution: Emerging views from comparative biology and geology. *Science*, *284*(5423), 2129–2137. https://doi.org/10.1126/science.284.5423.2129

Koenderink, J. J. (1986). Optic flow. *Vision Research*, *26*(1), 161–180.

Kountouriotis, G. K., Shire, K. A., Mole, C. D., Gardner, P. H., Merat, N., & Wilkie, R. M. (2013). Optic flow asymmetries bias high-speed steering along roads. *Journal of Vision*, *13*(10), 23–23. https://doi.org/10.1167/13.10.23

Kroll, V., & Crundall, D. (2019). Aperture judgement in fire-appliance drivers. *Transportation Research Part F: Traffic Psychology and Behaviour*, *63*, 55–66. https://doi.org/10.1016/j.trf.2019.03.012

Lee, D. N. (1976). A theory of visual control of braking based on information about time-to-collision. *Perception*, *5*, 437–459.

Lee, D. N. (1980). The optic flow field: The foundation of vision. *Philosophical Transactions of the Royal Society of London. B, Biological Sciences*, *290*(1038), 169–179. https://doi.org/10.1098/rstb.1980.0089

Lee, D. N., & Aronson, E. (1974). Visual proprioceptive control of standing in human infants. *Perception & Psychophysics*, *15*(3), 529–532. https://doi.org/10.3758/BF03199297

Lee, D. N., & Lishman, R. (1977). Visual control of locomotion. *Scandinavian Journal of Psychology*, *18*(1), 224–230.

Li, L., & Chen, J. (2010). Relative contributions of optic flow, bearing, and splay angle information to lane keeping. *Journal of Vision*, *10*(11), 16–16. https://doi.org/10.1167/10.11.16

Li, L., & Warren, W. H. (2000). Perception of heading during rotation: Sufficiency of dense motion parallax and reference objects. *Vision Research*, *40*(28), 3873–3894. https://doi.org/10.1016/S0042-6989(00)00196-6

Lishman, J. R., & Lee, D. N. (1973). The autonomy of visual kinaesthesis. *Perception*, *2*(3), 287–294. https://doi.org/10.1068/p020287

Loomis, J. M., & Knapp, J. M. (2003). Visual perception of egocentric distance in real and virtual environments. In L. J. Hettinger & M. W. Haas (Eds.), *Virtual and adaptive environments: Applications, implications, and human performance issues* (pp. 21–46). Lawrence Earlbaum Associates, Inc.

Lucaites, K. M. (2018). Aperture passability in novice walker users: The impact of action scaling above and beyond body scaling. *All Theses, Clemson University.* https://tigerprints.clemson.edu/all_theses_2860

Lucaites, K. M., Venkatakrishnan, R., Bhargava, A., Venkatakrishnan, R., & Pagano, C. C. (2020). Predicting aperture crossing behavior from within-trial metrics of motor control reliability. *Human Movement Science*, *74*, 102713. https://doi.org/10.1016/j.humov.2020.102713

Lucaites, K. M., Venkatakrishnan, R., Venkatakrishnan, R., Bhargava, A., & Pagano, C. C. (2020). Predictability and variability of a dynamic environment impact affordance judgments. *Ecological Psychology*, 1–20. https://doi.org/10.1080/10407413.2020.1741323

Maas, C. J. M., & Hox, J. J. (2005). Sufficient sample sizes for multilevel modeling. *Methodology, 1*(3), 86-92.

Machado-León, J. L., de Oña, J., de Oña, R., Eboli, L., & Mazzulla, G. (2016). Socio-economic and driving experience factors affecting drivers' perceptions of traffic crash risk. *Transportation Research Part F: Traffic Psychology and Behaviour*, *37*, 41–51. https://doi.org/10.1016/j.trf.2015.11.010

Moore, K. S., Gomer, J. A., Pagano, C. C., & Moore, D. D. (2009). Perception of robot passability with direct line of sight and teleoperation. *Human Factors: The Journal of the Human Factors and Ergonomics Society*, *51*(4), 557–570. https://doi.org/10.1177/0018720809341959

Muroi, D., & Higuchi, T. (2017). Walking through an aperture with visual information obtained at a distance. *Experimental Brain Research*, *235*(1), 219–230. https://doi.org/10.1007/s00221-016-4781-7

Pagano, C. C., Fitzpatrick, P., & Turvey, M. T. (1993). Tensorial basis to the constancy of perceived object extent over variations of dynamic touch. *Perception & Psychophysics*, *54*(1), 43–54. https://doi.org/10.3758/BF03206936

Pagano, C. C., Kinsella-Shaw, J. M., Cassidy, P. E., & Turvey, M. T. (1994). Role of the inertia tensor in haptically perceiving where an object is grasped. *Journal of Experimental Psychology: Human Perception and Performance*, *20*(2), 276–285.

Pagano, C. C., & Turvey, M. T. (1998). Eigenvectors of the inertia tensor and perceiving the orientation of limbs and objects. *Journal of Applied Biomechanics*, *14*, 331–359.

Palatinus, Z., Carello, C., & Turvey, M. T. (2011). Principles of part–whole selective perception by dynamic touch extend to the torso. *Journal of Motor Behavior*, *43*(2), 87–93. https://doi.org/10.1080/00222895.2010.538767

Peng, C.-Y. J., Lee, K. L., & Ingersoll, G. M. (2002). An introduction to logistic regression analysis and reporting. *The Journal of Educational Research*, *96*(1), 3–14. https://doi.org/10.1080/00220670209598786

Petrucci, M. N., Horn, G. P., Rosengren, K. S., & Hsiao-Wecksler, E. T. (2016). Inaccuracy of affordance judgments for firefighters wearing personal protective equipment. *Ecological Psychology*, *28*(2), 108–126. https://doi.org/10.1080/10407413.2016.1163987

Prokop, T., Schubert, M., & Berger, W. (1997). Visual influence on human locomotion modulation to changes in optic flow: Modulation to changes in optic flow. *Experimental Brain Research*, *114*(1), 63–70. https://doi.org/10.1007/PL00005624

Reed, E. S. (1996). *Encountering the world: Toward an ecological psychology*. Oxford UNiversity Press.

Regan, D., & Beverley, K. I. (1982). How do we avoid confounding the direction we are looking and the direction we are moving? *Science*, *215*(4529), 194–196.

Rieser, J. J., Pick, H. L., Ashmead, D. H., & Garing, A. E. (1995). Calibration of human locomotion and models of perceptual-motor organization. *Journal of Experimental Psychology: Human Perception and Performance*, *21*(3), 480.

Riley, M. A., & Van Orden, G. C. (2005). *Tutorials in contemporary nonlinear methods in the behavioral sciences*. http://www.nsf.gov/sbe/bcs/pac/nmbs/nmbs.jsp

Sarre, G., Berard, J., Fung, J., & Lamontagne, A. (2008). Steering behaviour can be modulated by different optic flows during walking. *Neuroscience Letters*, *436*(2), 96–101. https://doi.org/10.1016/j.neulet.2008.02.049

Schubert, M., Prokop, T., Brocke, F., & Berger, W. (2005). Visual kinesthesia and locomotion in Parkinson's disease. *Movement Disorders*, *20*(2), 141–150. https://doi.org/10.1002/mds.20281

Snijders, T. A., & Bosker, R. J. (2012). *Multilevel analysis: An introduction to basic and advanced multilevel modeling* (2nd ed.). SAGE publications.

Solini, H. M., Bhargava, A., & Pagano, C. C. (2021). The effects of testing environment, experimental design, and ankle loading on calibration to perturbed optic flow during locomotion. *Attention, Perception, & Psychophysics*, *83*(1), 497–511. https://doi.org/10.3758/s13414-020-02200-1

Srinivasan, M. V. (1992). How bees exploit optic flow: Behavioural experiments and neural models. *Philosophical Transactions of the Royal Society of London. Series*

B: Biological Sciences, *337*(1281), 253–259. https://doi.org/10.1098/rstb.1992.0103

Srinivasan, M. V. (1998). Insects as Gibsonian animals. *Ecological Psychology*, *10*(3–4), 251–270.

Srinivasan, M. V., Lehrer, M., Kirchner, W. H., & Zhang, S. W. (1991). Range perception through apparent image speed in freely flying honeybees. *Visual Neuroscience*, *6*(5), 519–535. https://doi.org/10.1017/S095252380000136X

Turvey, M. T. (1992). Affordances and prospective control: An outline of the ontology. *Ecological Psychology*, *4*(3), 173–187. https://doi.org/10.1207/s15326969eco0403_3

Turvey, M. T. (2019). *Lectures on perception: An ecological perspective*. Routledge.

Turvey, M. T., Shaw, R. E., Reed, E. S., & Mace, W. M. (1981). Ecological laws of perceiving and acting: In reply to Fsdor and Pylyshyn. *Cognition*, *9*, 237–304.

Wagman, J. B., & Carello, C. (2003). Haptically creating affordances: The user-tool interface. *Journal of Experimental Psychology: Applied*, *9*(3), 175–186. https://doi.org/10.1037/1076-898X.9.3.175

Wagman, J. B., Langley, M. D., & Higuchi, T. (2017). Turning perception on its head: Cephalic perception of whole and partial length of a wielded object. *Experimental Brain Research*, *235*(1), 153–167. https://doi.org/10.1007/s00221-016-4778-2

Wagman, J. B., & Malek, E. A. (2007). Perception of whether an object can be carried through an aperture depends on anticipated speed. *Experimental Psychology*, *54*(1), 54–61. https://doi.org/10.1027/1618-3169.54.1.54

Wagman, J. B., & Taylor, K. R. (2005). Perceiving affordances for aperture crossing for the person-plus-object system. *Ecological Psychology*, *17*(2), 105–130.

Wagner, H. (1982). Flow-field variables trigger landing in flies. *Nature*, *297*(5862), 147–148. https://doi.org/10.1038/297147a0

Wagner, H. (1986). Flight performance and visual control of flight of the free-flying housefly (Musca domestica L.) II. Pursuit of targets. *Philosophical Transactions of the Royal Society of London. B, Biological Sciences*, *312*(1158).

Wann, J. P., Rushton, S., & Mon-Williams, M. (1995). Natural problems for stereoscopic depth perception in virtual environments. *Vision Research*, *35*(19), 2731–2736. https://doi.org/10.1016/0042-6989(95)00018-U

Warren, W. H. (1988). Action modes and laws of control for the visual guidance of action. In *Advances in Psychology* (Vol. 50, pp. 339–379). Elsevier. https://doi.org/10.1016/S0166-4115(08)62564-9

Warren, W. H. (1998). Visually controlled locomotion: 40 years later. *Ecological Psychology*, *10*(3–4), 177–219. https://doi.org/10.1080/10407413.1998.9652682

Warren, W. H. (2006). The dynamics of perception and action. *Psychological Review*, *113*(2), 358–389. https://doi.org/10.1037/0033-295X.113.2.358

Warren, W. H., & Fajen, B. R. (2004). From optic flow to laws of control. In L. M. Vaina, S. A. Beardsley, & S. K. Rushton (Eds.), *Optic Flow and Beyond* (pp. 307–337). Springer Netherlands. https://doi.org/10.1007/978-1-4020-2092-6_14

Warren, W. H., Kay, B. A., & Yilmaz, E. H. (1996). Visual control of posture during walking: Functional specificity. *Journal of Experimental Psychology: Human Perception and Performance*, *22*(4), 818–838.

Warren, W. H., & Whang, S. (1987). Visual guidance of walking through apertures: Body-scaled information for affordances. *Journal of Experimental Psychology: Human Perception and Performance*, *13*(3), 371.

Willemsen, P., Gooch, A. A., Thompson, W. B., & Creem-Regehr, S. H. (2008). Effects of stereo viewing conditions on distance perception in virtual environments. *Presence: Teleoperators and Virtual Environments*, *17*(1), 91–101. https://doi.org/10.1162/pres.17.1.91

Wilmut, K., & Barnett, A. L. (2010). Locomotor adjustments when navigating through apertures. *Human Movement Science*, *29*(2), 289–298. https://doi.org/10.1016/j.humov.2010.01.001

Wilmut, K., Du, W., & Barnett, A. L. (2015). How do I fit through that gap? Navigation through apertures in adults with and without Developmental Coordination Disorder. *PLOS ONE*, *10*(4), e0124695. https://doi.org/10.1371/journal.pone.0124695

Winter, D. A. (2005). *Biomechanics and motor control of human movement* (3rd ed.). Wiley.

Woltman, H., Feldstain, A., MacKay, J. C., & Rocchi, M. (2012). An introduction to hierarchical linear modeling. *Tutorials in Quantitative Methods for Psychology*, *8*(1), 52–69. https://doi.org/10.20982/tqmp.08.1.p052

Yilmaz, E. H., & Warren, W. H. (1995). Visual control of braking: A test of the r hypothesis. *Journal of Experimental Psychology: Human Perception and Performance*, *21*(5), 996–1014.

Zhao, H., & Warren, W. H. (2015). On-line and model-based approaches to the visual control of action. *Vision Research*, *110*, 190–202. https://doi.org/10.1016/j.visres.2014.10.008